SAE International

2012-01-0577
Published 04/16/2012
doi:10.4271/2012-01-0577
saecomveh.saejournals.org

Moving Deformable Barrier Test Procedure for Evaluating Small Overlap/Oblique Crashes

James Saunders, Matthew Craig and Daniel Parent
NHTSA

ABSTRACT

In September 2009 the National Highway Traffic Safety Administration (NHTSA) published a report that investigated the incidence of fatalities to belted non-ejected occupants in frontal crashes involving late-model vehicles. The report concluded that after exceedingly severe crashes, the largest number of fatalities occurred in crashes involving poor structural engagement between the vehicle and its collision partner, present in crashes characterized as corner impacts, oblique crashes, impacts with narrow objects, and heavy vehicle underrides. By contrast, few if any of these 122 fatal crashes were full-frontal or offset-frontal impacts with good structural engagement, excepting crashes that were of extreme severity or the occupants that were exceptionally vulnerable.

The intent of this research program is to develop a test protocol that replicates real-world injury potential in small overlap impacts (SOI) and oblique offset impacts (Oblique) in motor vehicle crashes. Previous work towards this goal has led to the development of a Research Moving Deformable Barrier-to-Vehicle (RMDBtV) test protocol, which is further evaluated in this paper. While there were some inherent differences in the Vehicle-to-Vehicle (VtV) and RMDBtV test results, the overall agreement of vehicle and occupant responses proved promising enough to perform another VtV to RMDBtV comparison. As in the previous study, the first step is to compare the RMDBtV to VtV test for the same vehicle. This comparison focuses on the target vehicle crash metrics (pulse shape, average deceleration, slope of the velocity time-history, total change in velocity, exterior crush profile, and interior intrusion) as well as occupant kinematics and injury assessment values.

The second step of this research program is to assess the performance of new vehicles in the SOI RMDBtV and the Oblique RMDBtV test procedures. This research will provide insight on the ability of these two test procedures to replicate vehicle and occupant response as seen in the field. This paper presents the results of 7 different 2010-2011 model year vehicles tested in both the SOI and the Oblique test procedures. In these tests the overlap and RMDB closing speed was held constant for both procedures. The vehicle response demonstrated a decreasing trend of delta-V and longitudinal acceleration with increasing vehicle mass, but the trend did not hold for lateral acceleration. Aside from the lightest vehicle showing the largest magnitude of intrusion, there was no apparent trend of vehicle mass with intrusion. The occupant kinematics demonstrated head contact locations that are common in the field, torso loading of the restraint system and steering wheel, and a distribution of injury assessment values that is representative of the field injury risk.

CITATION: Saunders, J., Craig, M. and Parent, D., "Moving Deformable Barrier Test Procedure for Evaluating Small Overlap/Oblique Crashes," *SAE Int. J. Commer. Veh.* 5(1):2012, doi:10.4271/2012-01-0577.

INTRODUCTION

According to a study conducted by Bean et al. in 2009 [1], poor structural engagement between the vehicle and its collision partner resulted in the largest number of fatalities to belted non-ejected occupants in frontal crashes involving late-model vehicles, excluding exceedingly severe crashes and/or anomalies. Motor vehicle crashes that demonstrate such poor structural engagement include corner impacts, oblique crashes, impacts with narrow objects, and heavy vehicle underrides. By contrast, few if any of these 122 fatal crashes were full-frontal or offset-frontal impacts with good structural engagement, unless the crashes were of extreme severity or the occupants were exceptionally vulnerable. As a result of the NHTSA study, the agency stated its intent to further analyze small overlap and oblique frontal crashes in its Vehicle Safety Rulemaking & Research Priority Plan 2009-2011 published in November 2009 [2].

To better understand the injuries, injury source, and occupant kinematics in these small overlap impacts (SOI) and oblique offset impacts (Oblique), NHTSA performed a review of motor vehicle crashes included in the Crash Injury

Research and Engineering Network (CIREN) and National Automotive Sampling System Crashworthiness Data System (NASS-CDS) databases [3]. In this study, a total of 276 drivers were identified to be involved in crashes that were characterized as either left offset or SOI. Left offset was defined as having only the left longitudinal being engaged during the crash. SOI was defined as engagement outside the left longitudinal, as defined by Halloway et al. in 2011 [4]. Drivers sustained AIS 3+ injuries to the knee-thigh-hip (KTH) complex in 65% of the cases, AIS 3+ chest injuries in ~45% of the cases, AIS 2+ leg and foot injuries in ~38% of the cases, and AIS 3+ head injuries in ~19% of the cases. There was no consistent and significant difference in the injury distribution between left offset and SOI. The most frequent source of KTH injury was contact to the instrument panel, responsible for 80% of the AIS 3+ KTH injuries sustained in left offset and SOI. The attribution of chest injury source varied noticeably by crash mode, and was divided between interaction with the safety belt (47% left offset, 39% SOI), steering wheel (34% left offset, 16% SOI), and door (9% left offset, 31% SOI). Sources for AIS 3+ head injuries were distributed over a wide range of contact surfaces, including the steering wheel (32%), A-pillar (~17%), and air bag (~9%).

NHTSA initiated a research program to investigate crash test protocols that replicates real-world injury potentials in small overlap (SOI) and oblique frontal offset impacts. The main objective of this research program was to develop a test procedure involving a moving deformable barrier (MDB) in order to a) allow comparisons of vehicles across classes, b) reduce the costs that would be associated with vehicle-to-vehicle test procedures, and c) create a feasible test procedure that could be reproduced a wide number of crash test facilities.

The first step in this program was to conduct VtV tests in both SOI and Oblique conditions, which could subsequently be used as surrogates to evaluate the utility of MDB-to-vehicle crash tests. Paired VtV and MDBtV tests in the oblique condition were carried out for three passenger cars (PC): PC weighing 1731 kg (PCa), PC weighing 1892 kg (PCb), and a smaller PC weighing 1345 kg (PCc). Additionally, paired VtV and moving deformable barrier-to-vehicle (MDBtV) tests were carried out in the SOI condition for the PCa and the PCc. Evaluation of these tests led to improvements to the Federal Motor Vehicle Safety Standards (FMVSS) No. 214 Side Impact Protection MDB that was originally implemented, resulting in the Research Moving Deformable Barrier (RMDB). The previous study by Saunders et al. in 2011 [5] presented the results of VtV, MDBtV, and RMDBtV tests of a PCa in the SOI and oblique condition, as well as VtV and MDBtV tests of a PCb in the oblique condition. The current study contributes an additional RMDBtV test of a PCb in the oblique condition. Since the RMDB overrode all the vehicles in the SOI test configurations intended to replicate VtV SOI tests, no comparisons of the RMDBtV SOI will be presented in this paper.

Additionally, a series of 15 RMDBtV tests (8 SOI and 7 Oblique) were conducted to assess the performance of 2010 and 2011 model year vehicles. In this paper this test series is referred to as "New Model Tests." This test series included different classes of vehicles, including a sub-compact car on the light end and full-size truck on the heavy end. This test series was performed to provide insight into the ability of these two test procedures to represent the vehicle crash characteristics and occupant injury risk seen in the field. In order to compare vehicles across classes, the New Model Tests used a constant-energy test configuration with a constant impact speed for the RMDB.

TEST PROCEDURE DEVELOPMENT

From the Rudd analysis [3] of real world cases, it was suggested that the steering wheel-mounted air bag did not properly restrain the occupant, and the head often moved outboard of the air bag to contact the A-pillar or upper portion of the door. Therefore, NHTSA chose the Test Device for Human Occupant Restraint (THOR) anthropomorphic test device (ATD) for this crash test program. The THOR-NT, as described by Shams et al. in 2005 [8], has advanced biofidelity and instrumentation features that were thought to be useful for the current study. From a biofidelity perspective, the THOR-NT has a more flexible spine and improved neck biofidelity compared to other 50th percentile dummies, allowing for kinematics that may better represent those of a human. Among other instrumentation advantages of the THOR-NT, it has the capability of measuring multi-point (four locations) chest deflection and bi-lateral, tri-axial acetabular loads. For all target vehicles in this study, the THOR-NT 50th percentile male test dummy was positioned the driver's seat according to FMVSS No. 208 seating procedure.

In order to determine the test setup for Oblique test procedure, Saunders used the 2009 analysis from Eigen and Najm [7]. They studied 389 NASS CDS vehicles in frontal crashes that had an occupant who sustained a MAIS 3+ injury. The results of this study showed that 95 percent of the cases had a change in velocity or delta V (DV) below 60 kph, and 67 percent had an overlap of 50 percent or less. They also performed an analysis of 1998-2005 NASS-CDS cases which showed that 73 percent of vehicles with frontal damage were VtV. In a related non-published analysis of this data, it was found that while the highest percentage of MAIS 3+ cases involved a principal direction of force (PDOF) equal to 0 degrees, a significant percentage of MAIS 3+ cases involved a PDOF between 340 and 350 degrees. Using this information and additional computer modeling, Saunders [5] used the following test parameters for the Oblique VtV test procedure: (1) to simplify the test procedure since few crash test facilities that can perform an angled VtV crash test with both vehicles moving, the target vehicle was held stationary; (2) the bullet vehicle impacted the target vehicle at 113 kph

(70 mph); (3) the overlap of 50 percent was used to produce occupant compartment intrusion; and (4) the target vehicle was angled 15 degrees relative to the track to produce oblique kinematics of the dummy. To further simplify the test procedure, an Oblique MDBtV test condition was developed, where conservation of momentum was used to calculate an estimated DV in the target vehicle of 56 kph (35 mph) in a full frontal crash.

To determine the SOI test procedure, a collinear pole crash test was performed at the Medical College of Wisconsin (MCW). The NHTSA test number for this test is 7490 and can be downloaded from the NHTSA's Vehicle Crash Test Database[1]. In this test, the outside of the pole was aligned with the outside of the longitudinal of the target vehicle, with no initial vehicle rotation. The vehicle displaced laterally during the test to the point that it slid off of the pole before the occupant compartment was engaged. A subsequent test used an angle of 15 degrees (as used in the oblique procedure) as a means to produce better engagement in an attempt to match the intrusion patterns observed in the field data (NHTSA Test Number 7491). During this test, it was observed that the pole did not engage the structure of the vehicle outboard of the longitudinal rail as seen in the field, it instead penetrated toward the center of the vehicle. The conditions of these two tests were interpolated to arrive at an angle of 7 degrees for the SOI condition, in order to keep engagement while allowing the pole to penetrate outboard of the longitudinal rail. Using this information, the SOI test procedure was the same as the oblique procedure, with the exception of the target vehicle angle (7 degrees) and the amount of overlap, as the outsides of the left longitudinal rails of the target and bullet vehicles were aligned. To reproduce this SOI test in an MDB procedure, the following parameters were developed: (1) MDB aligned outside the rail; (2) closing speed of the MDB calculated using conservation of momentum to achieve a 56 kph (35 mph) DV in the target vehicle; and (3) the target vehicle rotated 7 degrees relative to the track.

The first set of tests using the FMVSS No. 214 MDB demonstrated several undesirable issues, as described by Saunders et al. in 2011 [5]. First, the 214 MDB honeycomb bottomed out too soon, causing a spike in the acceleration early in the event. Second, the tires of the 214 MDB were not protected by the face plate, causing unforeseen damage to the barrier. Finally, the use of 50 percent overlap procedure did not produce the same A-pillar intrusion as the VtV test. For these reasons, the moving deformable barrier was replaced by an instrumented barrier designed and developed by Trella et al., (2000) [9], which was originally developed for use in research crash testing to address vehicle aggressivity and compatibility issues. The instrumented MDB (iMDB) design is an adaptation of the current FMVSS No. 214 MDB design and duplicates as closely as possible its physical and dynamic specifications. This MDB also had the following features: (1) a suspension system to prevent bouncing of the cart during approach, (2) ability to ballast up to 2722 kg (6000 lbs), (3) adjustable ride height, (4) ability to adjust wheel base, and (5) can be used in both side and frontal impacts.

NHTSA further modified the MDB to widen the face plate to be outside of the track width of the barrier in order to protect the wheels of the barrier. Also, the face plate was lowered in an attempt to prevent override, and raised such that it was as high as the window sill for most vehicles. The honeycomb was modified to prevent bottoming out of the barrier too soon in the event. Using computer modeling, a two-layered barrier honeycomb face was developed. The first layer was 300 mm thick and had a stiffness of 0.724 MPa (100 psi) and the second layer was also 300 mm thick and the stiffness was increased to 1.71 MPa (245 psi) to prevent bottoming out of the barrier during the event. The resulting barrier is referred to as the Research Moving Deformable Barrier (RMDB). It should be noted that the design characteristics (i.e. frontal stiffness) of the RMDB were not developed to match a specific or even an average passenger car, but were developed to address the issues observed in testing with the FMVSS No. 214 MDB. Since the RMDB is homogenous, the barrier would more evenly distribute the crash load on the struck vehicle where an actual vehicle produced more localized loading due to the longitudinal frame rails and engine. It was believed that changing the overlap from 50 percent to 35 percent would allow the RMDB to interact more like an actual bullet vehicle as it could better expose the A-pillar and instrument panel to more of the crash forces.

From the previously-published tests [5], it was demonstrated that compared to the oblique FMVSS No. 214 MDB, the Oblique RMDBtV improved the qualitative and quantitative agreement of the target vehicle acceleration pulse compared to its VtV counterpart in the case of a PCa. While there were some differences in the A-pillar intrusion and resulting occupant response, the comparison was promising. However, when implemented in the SOI condition, the RMDB overrode the PCa. NHTSA also performed SOI VtV (NHTSA Test Number 7293) and Oblique VtV (NHTSA Test Number 7371) tests with the PCc to have a comparison of a compact car when using the RMDB. However, when these tests were repeated with the RMDB in both the Oblique (NHTSA Test Number 7434) and SOI (NHTSA Test Number 7433) configurations, the RMDB overrode the target vehicle in both cases. Therefore, the face plate was lowered to its lowest position possible. Figure 1 shows the final dimensions of the RMDB used in this paper.

---

[1] http://www-nrd.nhtsa.dot.gov/database/aspx/vehdb/querytesttable.aspx

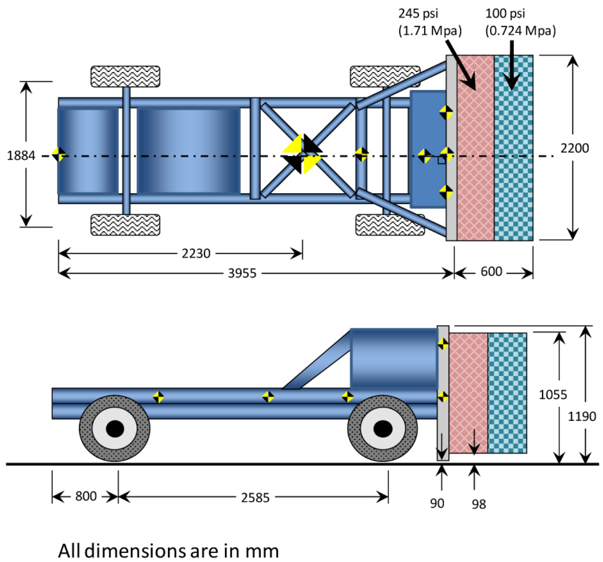

Figure 1. Dimensions of the RMDB

RMDBTV TO VTV COMPARISON

VEHICLE RESPONSE METHODOLOGY

The vehicle characteristics used for evaluation of the RMDBtV test relative to the VtV test, are listed below.

1. The acceleration pulses (shape, peak Gs, peak Gs timing, average deceleration, and duration). Since the target vehicle is stationary, there is not always a point where the acceleration crosses zero during the main part of the event. For this paper, the duration is defined as the time it takes the acceleration pulse to go above −10 Gs after peak Gs is reached (duration$_{-10Gs}$). Sometimes there are oscillations in the acceleration when the acceleration was around −10 Gs. In this case, the latest part of the acceleration was used for analysis. Saunders et al. (2007) [6] showed that average deceleration (AvgGs) is a good predictor of probability of injury and was defined as the closing speed divided by the time it takes for the velocity to cross zero. Again, since the vehicle is stationary and time to zero crossing of the velocity trace cannot be determined, duration$_{-10Gs}$ replaces the time to zero crossing of the velocity. Also, the closing speed is replaced by the change in velocity at duration$_{-10Gs}$ (DV$_{-10Gs}$). Equation 1 was used to calculate AvgGs$_X$ in the longitudinal direction. Since the magnitude of the lateral acceleration is less than the longitudinal acceleration the AvgGs$_Y$ is calculated when the acceleration goes below 5 Gs.

$$\text{AvgGs}_X = \frac{1000*1000*\text{DV}_{-10Gs}}{3600*9.81*\text{duration}_{-10Gs}} \tag{1}$$

2. The slope of the velocity time history and total DV.

3. Interior intrusion. A 4 by 5 matrix was placed on the toepan and floorpan and four points across the middle of the toepan (row 2, Figure 2) were used for the comparison analysis and all points are used latter in this paper. The procedure is as followed:

1. Locate and mark point D1 (column D row 1): Project a line 45 degrees (from the horizontal) down and forward from the center of the top accelerometer pedal in the x-z plane until the line intersects the interior of the vehicle. Mark this point by cutting a small “v” in the carpet and underlying padding and peeling back and exposing the floor. The carpet and padding are then refitted prior to crash.

2. ST plane: The ST plane is a y-z plane that passes through the front edge of the right seat track.

3. AP1 plane: The AP1 plane is a y-z plane that passes through point D1.

4. AP2 plane: The AP2 plane is an x-z plane that passes through point D1.

5. AP3 plane: The AP3 plane is an x-y plane that passes through point D1.

6. MP plane: The MP plane is a y-z plane located halfway between the ST plane and AP1 plane.

7. CF plane: The CF plane is an x-z plane that passes through the center of the footrest. If there is no visible footrest, locate the x-z plane to pass through a point located 64 mm measured along the MP plane in the y-direction from the intersection of the door sill and floorboard.

8. BP plane: The BP plane is an x-z plane that passes through the center of the brake pedal.

9. TP plane: The TP plane is a y-z plane at the intersection of the BP plane and the intersection of the toe pan and floorboard.

10. Column A is at the intersection of the vehicle and the CF plane.

11. Column D is at the intersection of the vehicle and the AP2 plane.

12. Row 1 is at the intersection of the vehicle and the AP3 plane.

13. Row 3 is at the intersection of the vehicle and the TP plane.

14. Row 5 is at the intersection of the vehicle and MP plane.

15. Columns B and C are evenly spaced between Columns A and D.

16. Row 2 is evenly spaced between Row 1 and Row 3.

17. Row 4 is evenly spaced between Row 3 and Row 5.

18. Map and mark additional driver points:

a. Mark the center of the brake pedal.

b. Mark the left upper IP located above where dummy's knees contact the dash.

c. Mark the right upper IP located above where dummy's knees contact the dash.

d. Mark the center of the steering wheel.

4. Mark the front outboard seat attachment point A-pillar bottom: A-pillar bottom intrusion is point 1 in the door profile measurements (Figure 3). The door profile and 4 by 5 matrix measurements will be used later in the paper and the procedures for obtaining these points are as followed:

a. Put steering wheel in center position. Create a horizontal plane (plane 1) that passes through the center of the steering wheel.

b. Point 1: Mark the sheet metal at the intersection of plane 1 and the outer edge of rubber part of the door sill running down the A-pillar.

c. Point 22: Mark the sheet metal at the intersection of plane 1 and the outer edge of rubber part of the door sill running down the B-pillar.

d. Mark 20 evenly spaced points between points 1 and 22 along the outer edge of the rubber door sill on the sheet metal.

e. Mark 20 evenly spaced points between points 22 and 1 along the outer edge of the rubber door sill on the sheet metal.

5. Exterior profile of the target vehicle. To obtain the exterior profile, the vehicle was placed at the proper attitude and a vehicle coordinate system was created at the rear bumper. The target vehicle is measured around the circumference of the vehicle at the height of the center of the bumper (d1) (Figure 4a). After the test, the vehicle was put back into its original vehicle coordinate and re-measured at the same height (d1) after the test (Figure 4b).

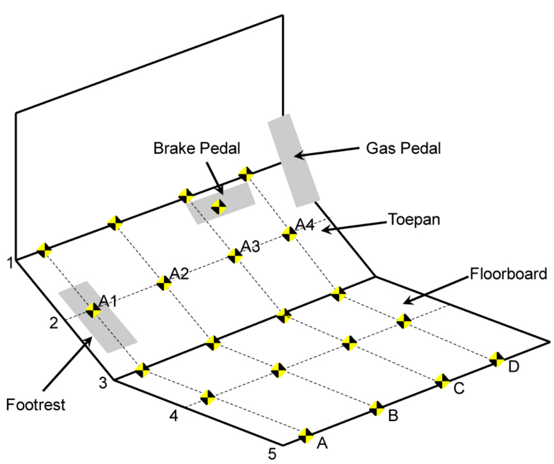

Figure 2. Toepan measurements

Figure 3. Door profile measurements

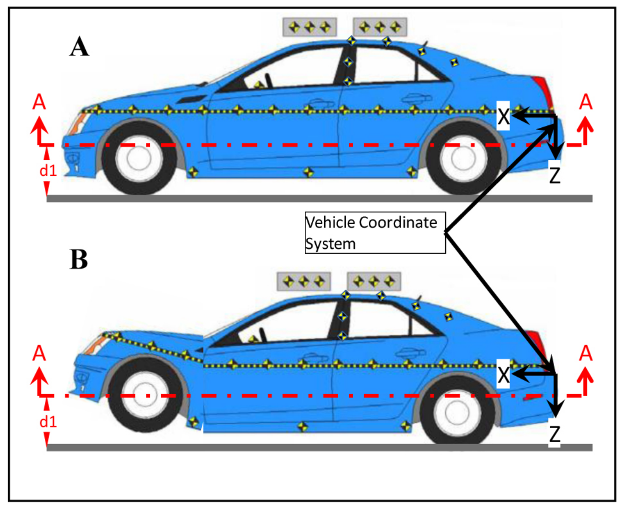

Figure 4. External crush profiles

OCCUPANT RESPONSE METHODOLOGY

For all of the tests presented in the current study, a THOR 50th percentile male anthropomorphic test device (ATD) was positioned in the driver's seat of the target vehicle. For the VtV and RMDBtV comparison tests, a standard THOR-NT ATD as described by Shams et al [8] was used. The THOR-NT ATD was instrumented with a nine-accelerometer array in the head to record six-degree-of-freedom kinematics, upper and lower neck loads and moments, accelerations of the thoracic spine and pelvis, three-dimensional displacements of four anterior rib cage locations measured using systems of rotational potentiometers and rigid links known as CRUX units, three-dimensional displacements of two anterior abdominal locations measured using double-gimballed string potentiometer (DGSP) systems, bi-lateral acetabulum loads, bi-lateral femur loads and moments, bi-lateral upper and lower tibia loads and accelerations, and ankle rotations.

While injury risk functions specific to the THOR hardware have not yet been developed [15], provisional injury assessment reference values have been developed for several body regions. To assess head injury risk, the head injury criterion (HIC) is assumed to be applicable to THOR, since the design requirements for the mass, moment of inertia, and biomechanical response characteristics mirror that of the Hybrid III for which HIC is traditionally applied. Additionally, a rotational brain injury criterion (BRIC) has been developed to estimate the risk of brain injury due to rotation of the skull [9]. Further test data are necessary to fully develop the relationship between BRIC and cumulative strain damage measure (CSDM) specific to THOR, but for the purpose of this analysis all of the THOR tests in the small overlap and oblique test program have been used to develop the intercepts (63.5 rad/s and 19,501 rad/s^2) for the calculation of BRIC for the tests presented in this paper (See Appendix B). The BRIC Injury Assessment Reference Value (IARV) is 0.89, which corresponds to a 30% risk of AIS 3+ traumatic brain injury (TBI). For the neck, cervical spine load tolerance values, which would represent a conservative estimate of tolerance values when applied to the stiffer THOR neck, have been proposed: tension force of 2520 Newtons (N), compression force of 3640 N, flexion moment of 48 Newton-meters (Nm), and extension moment of 72 Nm [11]. Injury assessment reference values have not yet been determined for the THOR chest, though research has been planned to develop an injury risk function that leverages the ability of the THOR to measure deflection at four points on the anterior rib cage. The fracture tolerance of a human hip under neutral loading through the knee was determined to be 4560 N [12]; adjusting for the difference in load transfer between the THOR dummy and human subjects, the associated load measured at the THOR acetabulum would be 3500 N [13]. Lower extremity injury risk was assessed using the Revised Tibia Index, for which the IARV of 1.16 represents a 50% risk of an AIS 2+ leg shaft injury [14].

RESULTS RMDBTV TO VTV OBLIQUE COMPARISON

Vehicle Response: VtV vs. RMDBtV

The PCb was used for this RMBDtV to VtV comparison. Figure 5 shows the shape of the left rear sill acceleration of the PCb in the RBMDBtV test has a similar shape to the VtV left rear sill acceleration in both the x and y direction. The only difference in the RMDBtV X-acceleration compared to the VtV X-acceleration is that the RMDBtV X-acceleration is slightly higher, the peaks occur earlier, and the duration-10Gs of the pulse is shorter. The effect of this earlier acceleration can be seen in both the AvgGs$_X$ and the velocity trace (Figure 6) The AvgGs$_X$ are higher for the RMDBtV tests (≈ 4Gs) and the change in velocity starts sooner for the RMDBtV test. But it should be noted that RMDBtV velocity slope is similar to the VtV velocity slope. The Y-direction RMDBtV vehicle characteristics were similar in the Y-direction. Table A 1 and Table A 2 in the Appendix show all of the calculated vehicle characteristics in both the X- and Y-directions.

Figure 7 shows that the interior intrusions of the PCb RMDBtV compared to the VtV test. This figure shows the RMDBtV test has a similar toepan intrusion pattern, but at slightly different magnitudes. For the IP and Steering Wheel intrusions the RMDBtV intrusions were slightly higher compared to the VtV test. Also, in this figure it can be seen that the A-pillar bottom intrusion was higher in the VtV test when compared to the RMDBtV test.

Figure 8 shows the post-test exterior profiles for the RMDBtV and VtV tests. From this figure it can be seen that the exterior profiles are similar, except at the left side longitudinal. Figure 9 shows the deformation of the left side longitudinal. It can be seen from this figure that the left side longitudinal did not deform during the RMDBtV test.

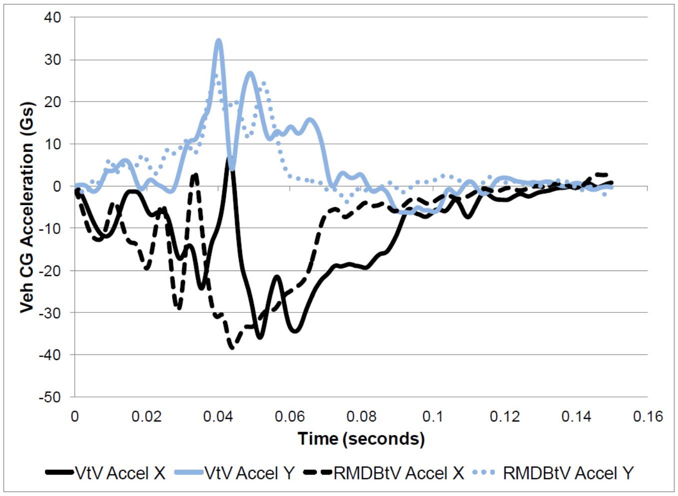

Figure 5. X and Y acceleration of the Oblique PCb

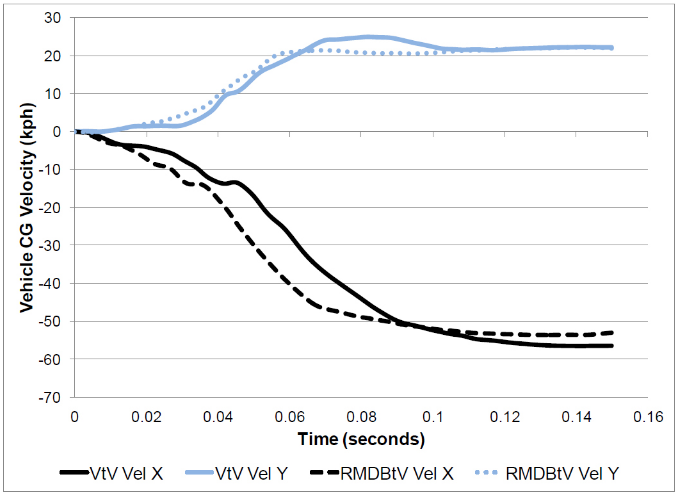

Figure 6. X and Y velocity of the Oblique PCb

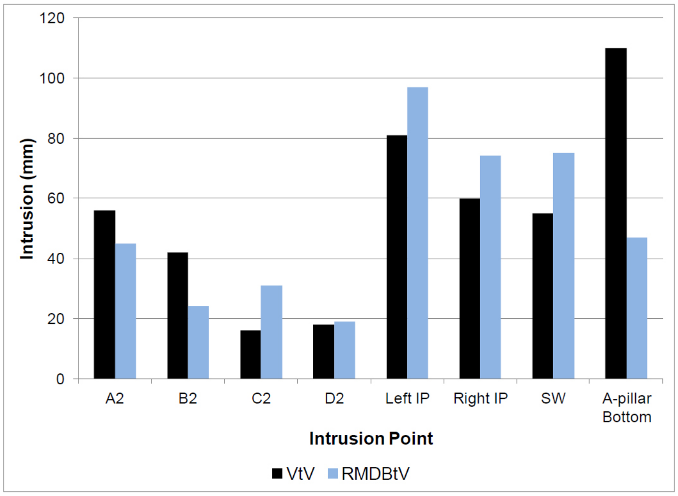

Figure 7. Interior intrusions of the Oblique PCb

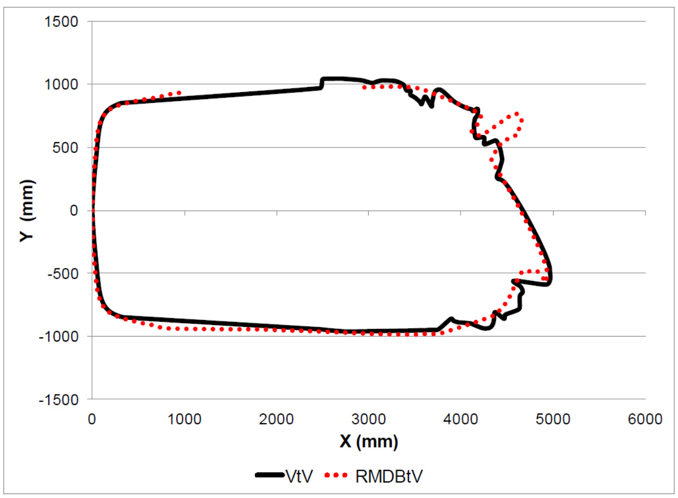

Figure 8. Exterior profile of the Oblique PCb

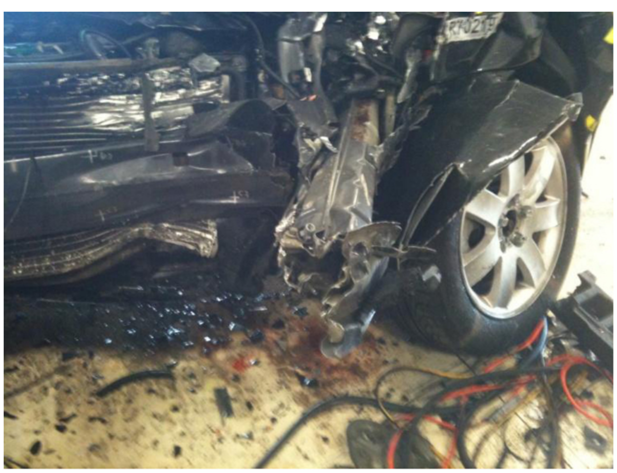

Figure 9. Oblique PCb main longitudinal structure not deformed

Occupant Response: VtV vs. Oblique RMDBtV

As reported by Saunders et al in 2011 [5], a comparison of VtV and RMDBtV Oblique tests was carried out using an exemplar mid-sized sedan (PCa) (NHTSA test numbers 6830 and 7366). The occupant kinematics in both test procedures were qualitatively similar, where the lateral acceleration pulse coupled with inboard deformation of the steering column resulted in the head slipping outboard of the air bag and translating towards the A-pillar. Due to differences in intrusion of the A-pillar as well as differences in the interaction of the torso with the restraint system, contact of the head with the A-pillar and door frame resulted in higher head accelerations in the VtV test than in the RMDBtV test. Differences in restraint interaction with the torso were also theorized to have contributed to differences in chest deflection and the magnitude and distribution of femur and acetabulum loads.

An additional RMBDtV test was performed using PCb (NHTSA test numbers 6831 and 7429) to allow further comparison to the VtV test procedure, which was carried out using PCb and presented by Saunders et al in 2011 [5].

The occupant kinematics in the PCb RMBDtV test were similar to those of the VtV test. The occupant initially translates forward parallel to the longitudinal axis of the vehicle, with an increasing outboard lateral component that begins to contribute about 50 milliseconds after the impact. The frontal air bag triggers at 22 milliseconds after initial bumper contact with the barrier, and the head of the occupant contacts left-of-center on the deployed air bag. After this initial air bag interaction, the steering assembly intrudes rearward (towards the occupant) and translates inboard. Since the occupant is moving outboard while the steering assembly is moving inboard, the occupant receives minimal restraint from the air bag and the head translates outboard towards the A-pillar and door frame. The head of the occupant contacts a similar location on the door panel in the vehicle-to-vehicle test (Figure 10) and RMBDtV test (Figure 11), though there are differences in the resulting head acceleration due to the structural deformation of the door. In the vehicle-to-vehicle test, deformation at the hinges causes the door to translate rearward and buckle outward (Figure 12), while in the RMBDtV test, the door frame approximately retains its original position and shape (Figure 13). This difference may have resulted in the elevated HIC_{15} measured in the RMBDtV test, as there was more structure immediately behind the door panel. Aside from the spike at the time of contact of the head with the door frame in the RMBDtV test, the resultant head accelerations are similar (Figure 14).

As with the comparison between the vehicle-to-vehicle and RMBDtV tests with the PCa, there were notable differences in the injury assessment metrics measured using the THOR dummy positioned in the driver's seat. The relevant injury assessment values (IAVs) are shown in Table 1, along with those from the previously-conducted relevant tests. Generally, the PCb RMBDtV test demonstrates higher values for all of the measured quantities compared to the vehicle-to-vehicle test, with the exception of abdominal deflection. While none of the provisional IARVs are exceeded in the vehicle-to-vehicle test, several are exceeded in the RMBDtV test (HIC15, BRIC, neck tension, left acetabulum resultant force, Tibia Index, and ankle rotation). However, the loading pattern appears to be similar, as the peak chest deflection occurs in the upper right quadrant in both tests, and the left aspect of the knee/thigh/hip (as measured at the acetabulum and femur) shows higher peak loads than the right aspect.

Comparing the thoracic response between vehicle-to-vehicle and RMBDtV, the magnitudes of the chest deflections are on average 15% higher in the RMBDtV tests. Correspondingly, belt loads are higher in each RMBDtV test compared to its paired vehicle-to-vehicle test (Figure 15). However, the trend in chest deflection among vehicles remains the same, as the peak occurred in the upper right quadrant for all four tests, and the peak chest deflection is higher in PCb than the PCa for both test conditions.

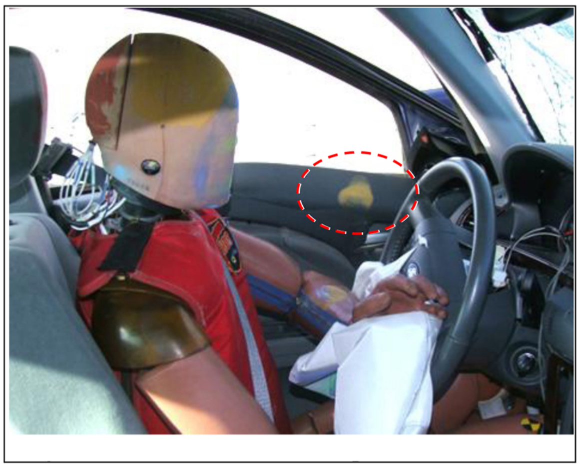

Figure 10. Head contact with door panel in PCb VtV test

Figure 11. Head contact with door panel in PCb RMBDtV test

Figure 12. Door frame deformation in PCb VtV test

Figure 13. Door frame deformation in PCb RMBDtV test

Table 1. Summary of occupant response in VtV and RMDB testing

Body Region	Metric	Location	Units	Ref.	PCa		PCb	
					VtV [6830]	RMDB [7366]	VtV [6831]	RMDB [7429]
Head	HIC15			700	594	233	361	2523
	BRIC			0.89	1.06	0.67	0.73	1.97
Neck	Tension	UNLC	N	2520	2767	2312	1808	3104
Chest	Deflection	UL	mm	N/A	18	20	24	34
	Deflection	UR	mm	N/A	31	36	42	51
	Deflection	LL	mm	N/A	-10	-14	-15	-12
	Deflection	LR	mm	N/A	-2	-3	35	-2
	Deflection	Peak	mm	N/A	31	36	42	51
	3ms Clip		g	60	36	49	32	44
Abdomen	Deflection	Peak	mm	111	36	13	44	39
Acetabulum	Force (Res.)	Left	N	3500	6236	4298	3376	3559
	Force (Res.)	Right	N	3500	1267	4474	1466	2014
Femur	Force (Axial)	Left	N	10000	5755	3538	4171	5301
	Force (Axial)	Right	N	10000	3910	7555	3472	4264
Tibia	Tibia Index	LU		1.16	0.45	1.34	0.33	0.78
Tibia	Tibia Index	RU		1.16	0.37	1.20	0.61	IM
Tibia	Tibia Index	LL		1.16	0.31	0.84	0.43	IM
Tibia	Tibia Index	RL		1.16	0.59	1.41	0.87	1.25
Tibia	Tibia Index	Max		1.16	0.59	1.41	0.87	1.25
Ankle	[in/e]version	Left	deg	35	16	IM	24	IM
Ankle	[in/e]version	Right	deg	35	35	36	31	28
Ankle	[p/d]flexion	Left	deg	35	36	61	29	39
Ankle	[p/d]flexion	Right	deg	35	40	45	34	25
Ankle	Rotation	Max	deg	35	40	61	34	39

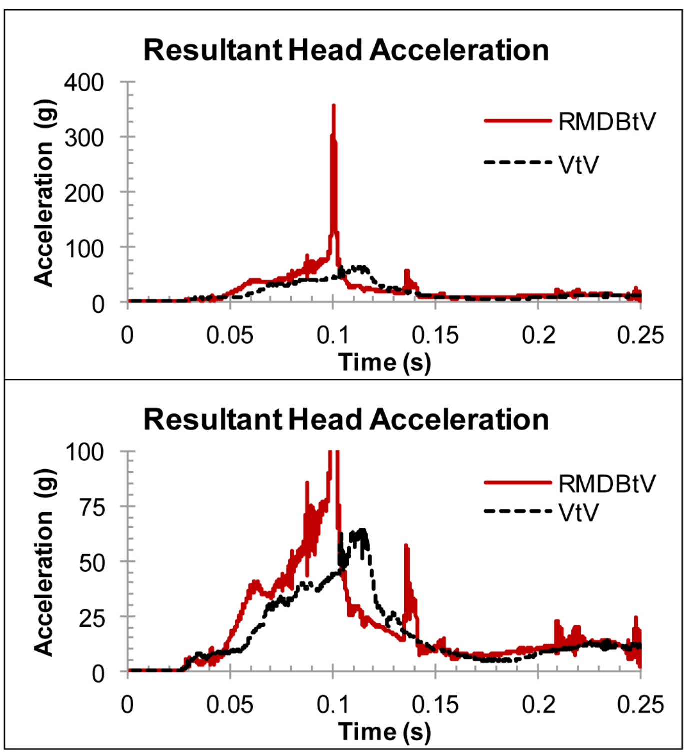

Figure 14. Head Acceleration in PCb VtV and RMBDtV tests. Top graph shows full range of the response, while the bottom graph disregards the point of impact with the door frame in the RMBDtV test.

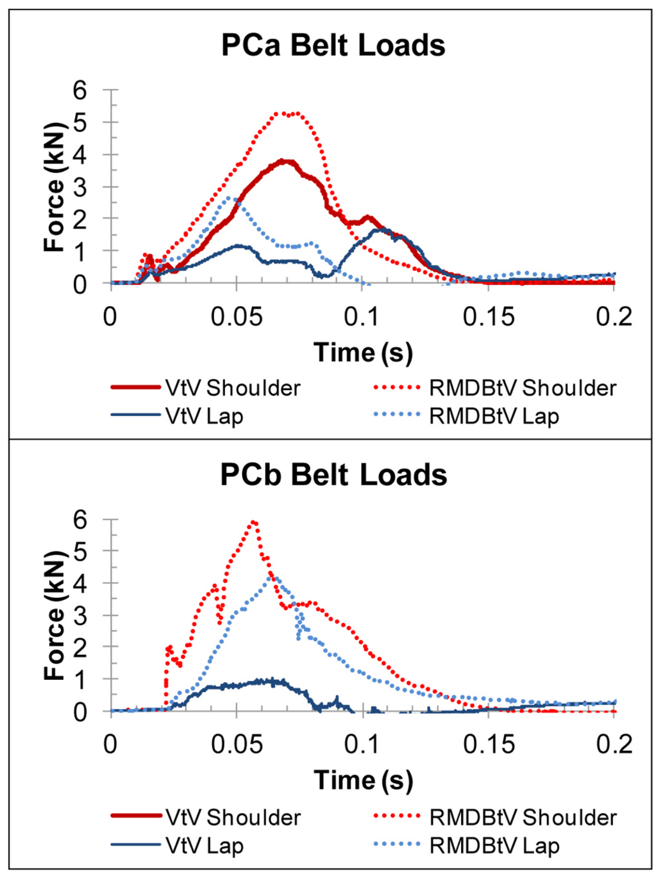

Figure 15. Shoulder and lap belt load time-histories for PCa and PCb VtV and RMDBtV tests. Note that the PCb VtV shoulder belt load cell experienced an equipment malfunction.

NEW MODEL TESTS

The fleet study was primarily designed to assess the viability of a constant-energy RMDBtV for both the SOI and the Oblique test procedure using 2010 and 2011 model year vehicles. Constant-energy means that every target vehicle is impacted by the RMDB at the same closing speed. This constant-energy method was chosen to be able to compare the performance of each vehicle across vehicle classes. Using conservation of momentum, the closing speed of the RMDB was calculated to be 90 kph (56 mph) based on the weight of the average 2011 passenger car and the weight of the RMDB. As mentioned above 95 percent of the case reviews had a DV below 60 mph and NHTSA wanted the average passenger car to have the same severity as the 90 kph (56 mph) frontal New Car Assessment Program.

The Oblique test procedure used in this study was the same as the RMDBtV to VtV comparison, except the closing speed of the RMDB was held constant. Since the final test procedure cannot rely on each test lab to uniformly locate the longitudinal rail of the target vehicle, a percent overlap needed to be determined for each SOI test. Halloway et al. (2011) determined the distance from the center of the vehicle to the center of the frame rail (d_{rail}) for different classes of vehicles, as well as the outer width of these vehicles. Using this information, the percent overlap to the d_{rail} from the outside of the vehicle was calculated and the statistics for these overlap are shown in Table 2. An overlap of 20 percent was selected for SOI testing such that the longitudinal rail would not be engaged for a majority of vehicles in the fleet.

The THOR-NT used in the fleet study was updated to include several structural and instrumentation modifications, known as the mod kit, intended to improve durability, usability, and biofidelity. While a full description of the modifications was covered by Ridella and Parent [15], several are summarized here due to their relevance to the small overlap and oblique crash modes. First, the head flesh was redesigned to achieve a constant thickness, which allows for a consistent impact response independent of the location of head contact. This proved to be important due to a wide range of head contacts that occurred to the A-pillar, steering wheel, and side window frame during this test series. Second, the instrumentation to measure chest deflection was modified in both form and function. In the THOR-NT CRUX system, both the upper and lower anterior sites are measured with respect to the spine component between the lumbar spine and the thoracic spine flex joints. In this arrangement, rotation about the thoracic spine flex joint without physical compression of the ribs can result in deflections as measured by the CRUX system. In the mod kit, each CRUX was replaced by a system using an Infrared Telescoping Rod for Assessment of Chest Compression (IR-TRACC) attached to the spine through two rotational potentiometers serving in a double-gimballed arrangement. In addition to reducing the propensity for instrumentation and human operator error, the IR-TRACC units resolved the issue of the interference of the CRUX linkage with the interior surface of the ribs. Furthermore, the deflection of the upper rib cage sites is measured from the upper thoracic spine segment, which prevents artifactual measurement of deflection due to rotation at the thoracic spine flex joint. Finally, the biofidelity of the femurs in axial compression has been improved, allowing for a more human-like response as well as the ability to apply human injury tolerance directly to measured loads and moments.

Eight vehicles were chosen for this study, ranging from lightest passenger car (PC) to the heaviest SUV/Pickup (PU) (Table 3). The main criterion for vehicle selection was that the vehicle chassis was redesigned or introduced in 2010 or 2011. However, there were three exceptions that did not meet this criterion. First, in order to account for the lightest vehicles in the current fleet, PC1 was chosen even though its design was introduced before 2010. Second, since PC2 was tested with a previous iteration of the RMDB, it was also included in the New Model Test series to ensure that lowering the face plate of the RMDB would prevent override. Third, PC5 was selected since this vehicle yielded interesting results from previous testing in a similar crash condition, as reported by Mueller et al in 2011 [17]. Seven of the vehicles were tested in both the SOI and the Oblique test procedure to investigate the difference in performance of a vehicle in these two crash modes.

Table 2. Statistics of overlap calculate for different classes of vehicles

	Overlap (%)
Maximum	30.4
Minimum	19.6
Average	24.5
Standard Deviation	3.4

Table 3. Fleet Study Test Matrix

Vehicle	Test Weight (kg)	SOI Test Number	Oblique Test Number
PC1	1033	7459	7458
PC2	1332	7444	7441
PC3	1365	7427	7428
PC4	1643	7432	7431
PC5*	1700	7430	Not Tested
PC6	1936	7468	7467
SUV1	2362	7426	7476
PU1	2611	7456	7457

**Only tested in the SOI condition*

RESULTS OF NEW MODEL TESTS

Vehicle Response: New Model Tests SOI

Figure 16 shows the differences of the velocity time history for each vehicle tested using the SOI test procedure. The vehicle with the highest total DV was the PC1 64 kph (40 mph) and the vehicle with the lowest was the PU1 43.5 kph (27 mph). Also, the time each velocity trace reached −10 kph ranged from 16.4 ms to 47.7 ms. Figure 17 shows the AvgGs for the X and Y direction for each vehicle. The chart is arranged from the lightest to heaviest vehicle. There is a decreasing trend in the AvgGs in the X-direction with increases in weight of the vehicle, but this trend does not hold for the AvgGs in the Y-direction.

Figure 18 shows the range of interior intrusions for the vehicles tested. In this figure the maximum X intrusion of any point measured for each region of the vehicle is used instead of the intrusion points used in the RMDBtV to VtV comparison. Also, the bars are arranged from lightest to heaviest vehicle. Aside from the lightest vehicle showing the highest or second highest intrusion in each measurement location, there was no apparent trend in intrusion versus the weight of the vehicle. The highest toepan intrusion occurred in the heaviest vehicle (PU1).

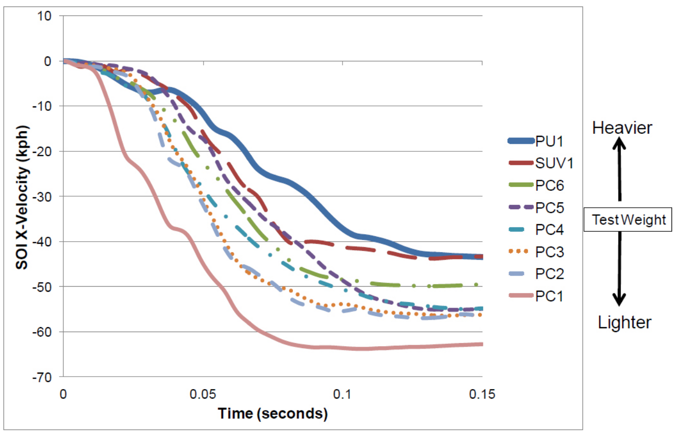

Figure 16. Left rear sill Velocity trace for SOI New Vehicle Tests

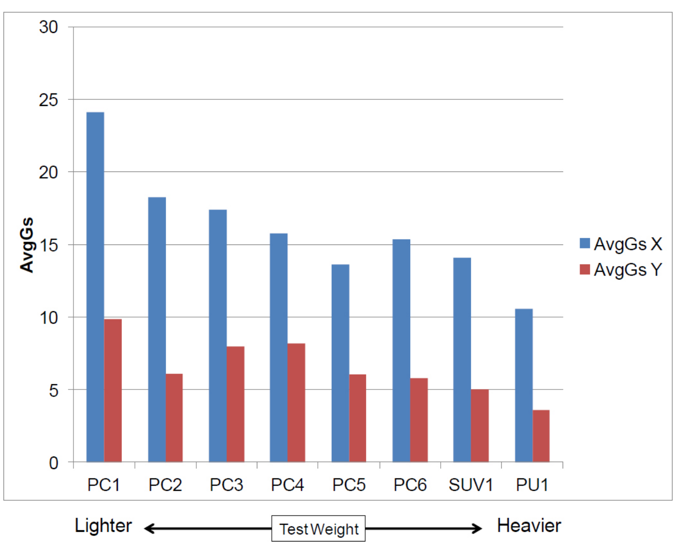

Figure 17. Left rear sill AvgGs for SOI New Vehicle Tests

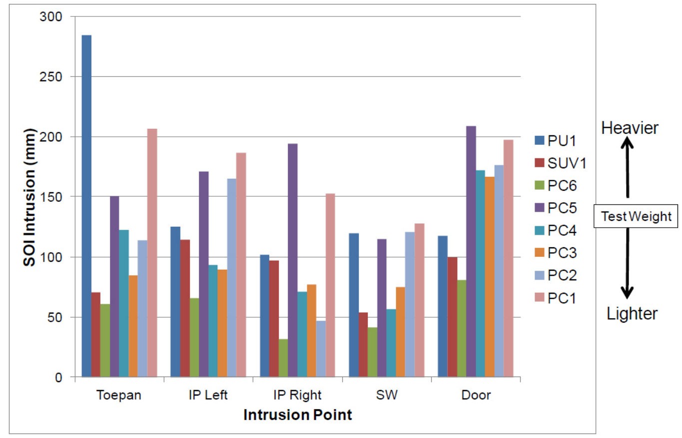

Figure 18. Interior intrusions for Small Overlap New Vehicle Tests

Vehicle Response: New Model Tests Oblique

Figure 19 shows the differences of the velocity time history for each vehicle tested using the Oblique test procedure. The vehicle with the highest total DV was the PC1 60.5 kph (37.5 mph) and the vehicle with the lowest was the SUV1 35.8 kph (22.2 mph). Also, the time each velocity trace reached −10 kph ranged from 15 ms to 35 ms. Figure 20 shows the AvgGs for the X and Y direction for each fleet vehicle. The chart is arranged from the lightest to heaviest weighted vehicle. There is a decreasing trend in the AvgGs in the X-direction with increases in weight of the vehicle, but this trend does not hold for the AvgGs in the Y-direction. Table A 1 and Table A 2 shows all the calculated vehicle characteristics.

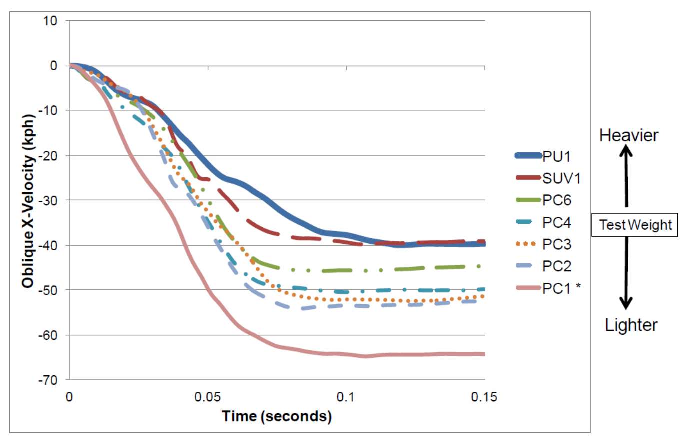

Figure 19. Left rear sill velocity trace for oblique New Vehicle Tests (Used VehCG))*

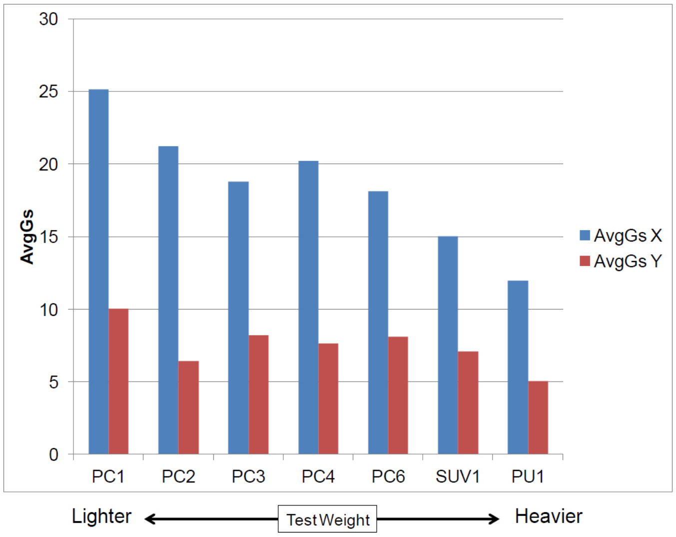

Figure 20. Left rear sill AvgGs for Oblique New Vehicle Tests (* Used VehCG)

Figure 21 shows the range of interior intrusions for the vehicles tested. In this figure the maximum X intrusion of any point measured for each region of the vehicle. Also, the bars are arranged from lightest to heaviest vehicle. Aside from the large magnitude of intrusion seen in the PC1, the lightest vehicle, there is no apparent trend of intrusion versus the weight of the vehicle.

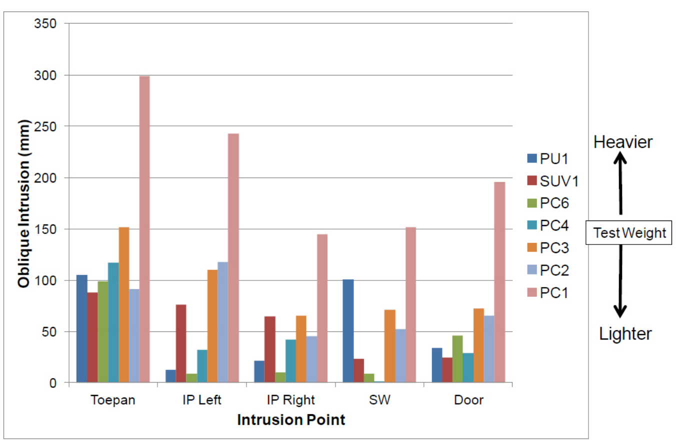

Figure 21. Interior intrusions for Oblique New Vehicle Tests

Occupant Response: New Model Tests SOI and Oblique

The kinematics of the occupant seated in the driver's seat followed the same general patterns in all of the SOI and Oblique vehicle tests. The occupant began moving directly forward with a gradually-increasing translation outboard. By the time the head of the occupant reached the air bag, there was sufficient lateral motion that the head slid or rolled off of the air bag restraint and continued translating towards the junction of the A-pillar and the door frame. There was at least some degree of intrusion of the steering column into the occupant compartment, and generally the air bag rotated upward and inward during the interaction with the head and torso of the occupant. Contact between the head and the air bag occurred in all tests (both SOI and Oblique), though the point of contact with the air bag fluctuated from center to upper left corner (Table 4).

In three of the tests (PC3 SOI, PC2 Oblique, PC3 Oblique), the head contacted the roof rail near the intersection with the top of the A-pillar, though only in the case of the PC3 SOI did this contact result in the highest HIC_{15} of the event. In four of the tests (PC2 SOI, PC2 Oblique, SUV1 Oblique, and PU1 Oblique), the head contacted the door frame at the point of peak forward, outboard, and downward excursion. There were three cases that exceeded the provisional IARV (700) for HIC_{15}: PC3 SOI, in which the head contacted the roof rail; PC2 Oblique, in which the head contacted the arm when it was adjacent to the door frame at the point of peak excursion; and SUV1 Oblique, in which the head contacted the door frame at the point of peak excursion. The resultant head acceleration time-histories in these three impacts show similar characteristics: a short-duration spike, resulting in a provisional HIC_{15} calculation window of 4 milliseconds or less (Figure 22).

In addition to the HIC_{15} injury assessment metric, the BRIC was calculated for each occupant to assess the risk of injury associated with rotational velocity and acceleration of the head. The provisional IARV for BRIC was exceeded for all of the fleet tests except for the PC4 Oblique, PC6 SOI, and SUV1 SOI tests. In this test condition, there are several modes of occupant kinematics that result in rotation of the head: interaction with the air bag, interaction with the side curtain air bag, and contact with the instrument panel, door frame, or roof rail. In most of the tests, the greatest angular velocity is imparted on the head during interaction with the air bag, since the head contacts the air bag while it is translating forward and outboard. This interaction results in a positive rotation about the local Z-axis of the head. The exceptions to this trend are cases that involved head impacts to the door frame, roof rail, or instrument panel, where the angular velocity of the head peaked later in the event. In these cases, the peak angular velocity of the head abruptly decreased at the time of impact, resulting in peak angular accelerations (Figure 23).

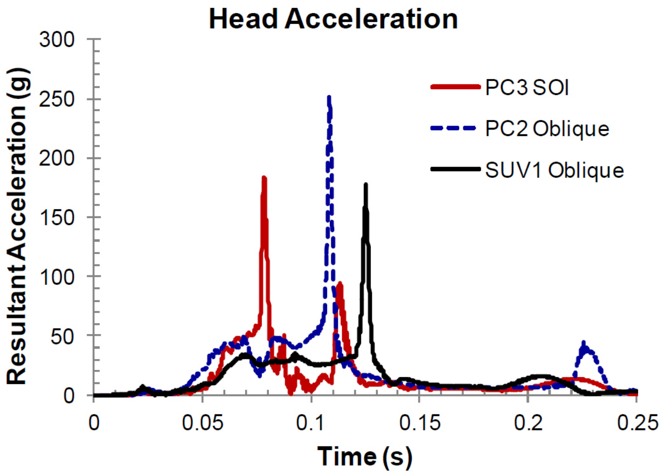

Figure 22. Resultant head acceleration time-histories of the three cases that exceeded the HIC15 provisional IARV.

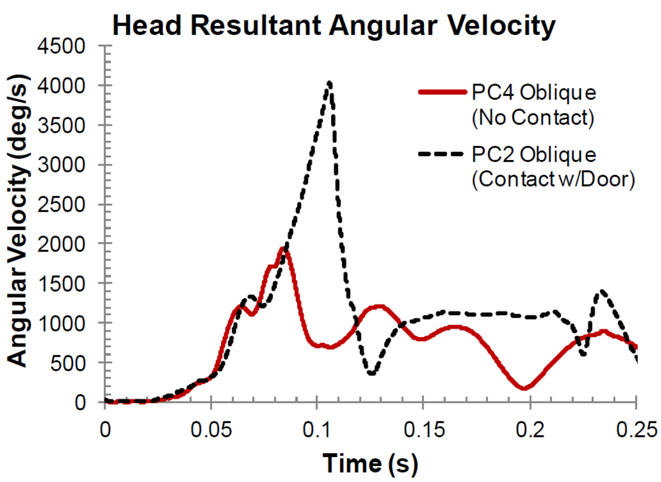

Figure 23. Resultant head angular velocity time-histories.

As the occupant translated forward and interacted with the restraint system, the torso of the occupant pitched forward about a lateral axis and rotated outboard about a longitudinal axis. As the head escaped the air bag in the outboard direction, the right side of the chest and the right shoulder interacted with the air bag and resulted in clockwise rotation (looking down on the vehicle) of the torso, and subsequently the pelvis, about a vertical axis. In all of the tests (both SOI and Oblique), the peak chest deflection occurred in either the upper right or the lower right quadrant of the chest, representing deflection of the 4^{th} and 8^{th} ribs respectively. Comparing SOI to Oblique crash modes, the location of peak chest deflection was the same for each vehicle pair except for the PU1. The PC1 and PC3 both showed peaks in the upper right, while the remaining vehicles showed peaks in the lower right. On average, the peak chest deflections measured in the Oblique test conditions were higher than those measured in the SOI conditions, though the average peak chest deflection in the Oblique tests was not outside of the standard deviation about the average of the SOI tests (Figure 24).

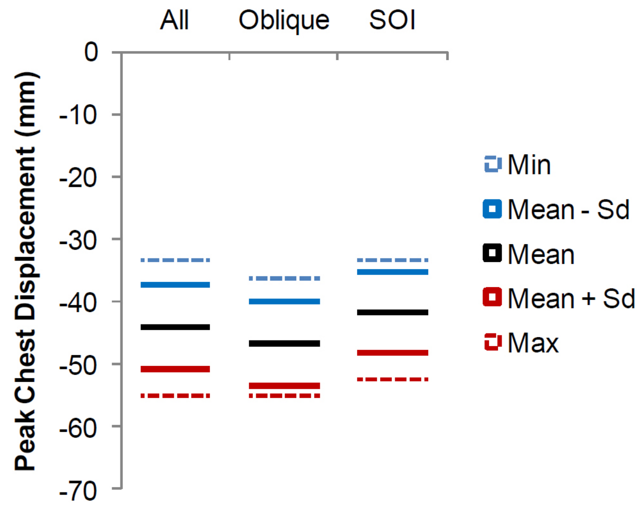

Figure 24. Mean, standard deviation, and overall range of peak chest deflection

The fleet tests demonstrated noticeable interaction of the restraint system with the abdomen. Peak abdominal deflections ranged from 52 to 74 millimeters, with similar magnitudes for the Oblique and SOI test conditions. In all cases except for the PC1 SOI, the peak abdominal deflection occurred on the right aspect of the abdomen. These peak deflections fall short of the provisional IARV for abdominal deflection, though the prediction of abdominal injury risk was not expected due to its low incidence in the field.

The knees and upper tibias of the occupant contacted the instrument panel and bottom of the steering column in all tests, though it was difficult to track the points of contact due to limited camera coverage and intrusion and damage to interior components during the crash. Both the intrusion and the biofidelic rotation of the pelvis may have contributed to the asymmetry of the loading, as nearly all test showed peak left acetabulum resultant loads that were higher than the right acetabulum resultant loads (excluding the PC2 Oblique, PC4 SOI, and tests where instrument malfunction prevented recording of one or more channels). Peak femur loads were also higher on the right side for these two exceptions, along with the PC3 Oblique test. Comparing SOI to Oblique, femur and acetabulum loads are on average less symmetric in the SOI condition.

The vehicle tests that showed the highest risk of lower extremity injury as predicted by the Revised Tibia Index metric were the PC1 (SOI and Oblique) and the PU1 SOI - the vehicles that showed the largest magnitudes of toepan intrusion. However, aside from these extremes, there was no apparent trend in toepan intrusion with lower extremity injury risk, as the vehicle that showed the smallest magnitude of toepan intrusion in the oblique condition was the PC6, which showed the 2^{nd}-highest Revised Tibia Index measurement of all oblique tests.

Table 4. Head contact locations and associated injury assessment values.

Mode	Vehicle	Contact Location: AB = Air Bag, SAB = Side Curtain Air Bag, RR = Roof Rail, IP = Instrument Panel, DP = Door Panel (Evidence): V = Video, PT = Paint Transfer	AD = Available and Deployed, AN = Available and Not Deployed, N = Not Available: Driver Air Bag	Side Curtain Air Bag	Peak HIC15
SOI	PC1	AB (V, PT)	AD	AN	285
	PC2	AB (V, PT); RR (V, PT); IP (V, PT); DP (PT)	AD	N	335
	PC3	AB (V, PT); RR (V, PT); SAB (V, PT)	AD	AD (80ms)	789
	PC4	AB (V); SAB (V, PT)	AD	AD (48ms)	121
	PC5	AB (V, PT)	AD	AD (38ms)	256
	PC6	AB (V, PT); SAB (V, PT)	AD	AD (36ms)	93
	SUV1	AB (V, PT); SAB (V, PT)	AD	AD (42ms)	54
	PU1	AB (V, PT)	AD	N	178
Oblique	PC1	AB (V, PT)	AD	AN	366
	PC2	AB (V, PT); DP (PT); RR (V, PT)	AD	N	1563
	PC3	AB (V, PT); RR (V, PT)	AD	AN	145
	PC4	AB (V); SAB (V)	AD	AD (50ms)	176
	PC6	AB (V, PT); SAB (V, PT)	AD	AD (12ms)	118
	SUV1	AB (V); DP (V, PT)	AD	AD (30ms)	703
	PU1	AB (V, PT); DP (PT)	AD	N	456

Table 5. Summary of occupant response in Oblique RMBDtV testing

Body Region	Metric	Location	Units	Ref.	Oblique PC1 [7458]	PC2 [7441]	PC3 [7428]	PC4 [7431]	PC6 [7467]	SUV1 [7476]	PU1 [7457]
Head	HIC15			700	366	1563	145	176	118	703	456
	BRIC			0.89	1.07	1.86	1.41	0.72	1.14	1.14	1.10
Neck	Tension	UNLC	N	2520		2164	1816	1476			
Chest	Deflection	UL	mm	N/A	18	17	22	14	16	23	14
	Deflection	UR	mm	N/A	47	42	46	33	34	38	34
	Deflection	LL	mm	N/A	-9	8	9	11	15	14	15
	Deflection	LR	mm	N/A	38	55	41	42	46	55	36
	Deflection	Peak	mm	N/A	47	55	46	42	46	55	36
	3ms Clip		g	60	57	54	45	35	42	41	32
Abdomen	Deflection	Peak	mm	111	54	63	65	52	52	56	53
Acetabulum	Force (Res.)	Left	N	3500	5043	2634		2938	4364	1574	2653
	Force (Res.)	Right	N	3500		2967	1588	2075	2574	1338	1951
Femur	Force (Axial)	Left	N	10000	9106	4373	2101	3150	6985	3202	4800
	Force (Axial)	Right	N	10000	8576	6267	2382	3006	3579	2732	3448
Tibia	Tibia Index	LU		1.16			0.49				
Tibia	Tibia Index	RU		1.16	2.79	0.83	0.58	0.54	1.84	0.57	0.72
Tibia	Tibia Index	LL		1.16	1.53	0.70		0.49	1.01	0.85	1.13
Tibia	Tibia Index	RL		1.16	3.24	1.11	0.87	0.71		0.46	0.85
Tibia	Tibia Index	Max		1.16	3.24	1.11	0.87	0.71	1.84	0.85	1.13
Ankle	[in/e]version	Left	deg	35	29	28	34	30	22		28
Ankle	[in/e]version	Right	deg	35	38	33	45	39	37	30	30
Ankle	[p/d]flexion	Left	deg	35	35	42	37	46	27	28	27
Ankle	[p/d]flexion	Right	deg	35	40	36	52	27	32	22	51
Ankle	Rotation	Max	deg	35	40	42	52	46	37	30	51

Table 6. Summary of occupant response in Small Overlap RMBDtV testing

Body Region	Metric	Location	Units	Ref.	Small Overlap Impact (SOI)							
					PC1 [7459]	PC2 [7444]	PC3 [7427]	PC4 [7432]	PC5 [7430]	PC6 [7468]	SUV1 [7426]	PU1 [7456]
Head	HIC15			700	285	335	789	121	256	93	54	178
	BRIC			0.89		1.25	1.64	1.02	0.91	0.84	0.84	0.90
Neck	Tension	UNLC	N	2520	2053	2041	2427	1688	2249		1179	1104
Chest	Deflection	UL	mm	N/A	11	21	12	20	24	18	20	13
	Deflection	UR	mm	N/A	34	51	40	35	40	31	38	33
	Deflection	LL	mm	N/A	6	-15	-9	11	-7	11	10	6
	Deflection	LR	mm	N/A	29	53	34	40	46	42	46	24
	Deflection	Peak	mm	N/A	34	53	40	40	46	42	46	33
	3ms Clip		g	60	46	56	52	35	52	38	32	31
Abdomen	Deflection	Peak	mm	111	54	58	71	53	74	57	52	44
Acetabulum	Force (Res.)	Left	N	3500	6949	5914	3549	1875	9340	2840	1666	2707
	Force (Res.)	Right	N	3500		2606	3024	2093	2148	1508	1531	2449
Femur	Force (Axial)	Left	N	10000	11646	9628	4904	2876	14994	4557	3019	4298
	Force (Axial)	Right	N	10000	7749	4366	1759	3538	3413	2877	2620	3525
Tibia	Tibia Index	LU		1.16			0.52				0.48	
Tibia	Tibia Index	RU		1.16	1.70	1.46		0.69	1.01	0.40	1.19	1.29
Tibia	Tibia Index	LL		1.16	2.30	1.06		0.77	0.80	0.48	0.24	2.97
Tibia	Tibia Index	RL		1.16	0.83	1.03	0.58	1.12	0.94	0.60	0.36	1.23
Tibia	Tibia Index	Max		1.16	2.30	1.46	0.58	1.12	1.01	0.60	1.19	2.97
Ankle	[in/e]version	Left	deg	35	28	25	29	28	18		25	27
Ankle	[in/e]version	Right	deg	35	32	34	42		32	37	44	34
Ankle	[p/d]flexion	Left	deg	35	27	16	24	32	49	33	23	40
Ankle	[p/d]flexion	Right	deg	35	16	13	15		16	24	9	36
Ankle	Rotation	Max		35	32	34	42	32	49	37	44	40

DISCUSSION

VTV AND RMDBTV COMPARISON

Vehicle Characteristics: VtV and RMDBtV Comparison

The objective of the RMBDtV test procedure described in this study is to drive the development of countermeasures to reduce the risk of fatalities and injuries that continue to occur in the field despite the modern advances in crashworthiness and advanced restraint systems in today's vehicle fleet. For a test procedure to be effective in driving the proper countermeasure development, it must accurately represent the real-world risk.

The small overlap and oblique research program was developed to demonstrate that a moving deformable barrier impact test procedure could represent the vehicle and occupant response in small overlap and oblique impacts seen in the field. The moving deformable barrier was selected for evaluation due to its repeatability and economy relative to vehicle-to-vehicle tests. The benefit of a fixed-mass, fixed-velocity moving deformable barrier test procedure is that comparisons across vehicle classes can be carried out. Additionally, such a procedure provides equalization in front-end stiffness where a fixed barrier test procedure might drive increases in stiffness of heavier vehicles that would hinder fleet compatibility.

In order to demonstrate the representativeness of the vehicle response in a moving deformable barrier condition, it is important to compare the response of the target vehicle in the crash test with the typical response of a vehicle in a real-world crash condition. Since there is a limited amount of information available to describe the vehicle and occupant response in the real-world crashes that result in injuries and fatalities, vehicle-to-vehicle tests were conducted as a surrogate. Two such vehicle-to-vehicle tests were carried out and evaluated: PCa and PCb, both in the oblique impact condition. Figure 25 shows a non-fatal Oblique CIREN (CIRENID-781129518) case of a vehicle similar to PCa into another PC. Even though the CIREN case appears more severe than the VtV crash test, it can be seen that the crush characteristics of the VtV are similar when compared to the CIREN case. The A-pillar buckles the same, the bumper crush is similar, and the tire is pushed back at the same angle.

Figure 25. Non-Fatal Oblique Case Comparison. Left picture is the CIREN case and right picture is PCa

Table 7 shows a set of vehicle characteristics and percent difference for both the Taurus and Five Hundred VtV and RMDBtV comparisons. It can be seen from this table that the percent differences between these vehicle parameters are similar for both the Taurus and the Five Hundred. In general the DV_{-10Gs} and $duration_{-10Gs}$ are less for the RMDBtV and the AvgGs are higher for the RMDBtV when compared to the VtV test. These differences likely stem from the fact that the RMDB is homogeneous, and its effective stiffness may be

Table 7. Vehicle Characteristics

	NHTSA Test Number	Test Type	DV-10Gs (kph)	Percent Difference	AvgGs	Percent Difference	Duration-10Gs	Percent Difference
	6830	VtV	50.8		12.7		113	
PCa	7366	RMDBtV	45.7	-10.0%	15.2	19.7%	85	-24.8%
	6831	VtV	50.1		15.6		90.8	
PCb	7429	RMDBtV	46.5	-7.2%	19.1	22.4%	69	-24.0%

greater than that of a typical vehicle. It also should be noted that the RMDB does not stay engaged to the target vehicle as long as the bullet vehicles does in the vehicle-to-vehicle tests.

In the PCb RMDBtV test the left side longitudinal rail did not deform as expected. This test indicates that it is possible that some longitudinal rails may simply penetrate the honeycomb of the MDB and not deform as seen in the real-world. However, this type of penetration of the barrier face was not seen in any of the other vehicles tested. Additionally, the change in velocity (Figure 6), peak intrusions (Figure 7) and exterior crush (Figure 8) are very similar for the PCb when comparing VtV and RMDBtV tests. Thus, the differences in rail deformation did not appear to significantly affect the overall results of the test.

Occupant Characteristics: VtV and RMDBtV Comparison

To assess the ability of the RMDBtV test procedure to represent the real-world occupant response in an oblique VtV crash, laboratory crash tests were conducted in the RMDBtV and VtV test conditions with a THOR-NT ATD in the driver's seat. Generally, the occupant kinematics and head trajectories were similar comparing the two test conditions for both a PCa and a PCb. However, due to differences in the A-pillar and door frame deformation, the location and severity of head impacts differed, with the PCa VtV showing a higher head injury risk than the PCa RMDBtV and vice-versa for the PCb tests. Relative to the occupant injury assessment metrics, the RMDBtV tests were more severe than the VtV counterpart for the peak chest deflection, 3ms clip chest acceleration, acetabulum resultant force (3 out of 4 cases), femur peak axial force (3 out of 4 cases), peak tibia index, and peak ankle rotation. Only the abdomen deflection showed values for the VtV condition that exceeded the values for the RMDBtV condition for both vehicles. In summary, the occupant response in the RMDBtV test condition did not exactly replicate the VtV condition, but showed similar enough trends in occupant kinematics and injury assessment values to warrant further examination of the RMDBtV test condition.

NEW MODEL TESTS

Vehicle Characteristics: New Vehicle Tests SOI and Oblique

Figure 26 shows the DV at −10ms for the x-direction and DV at 5ms for the y-direction. It can be seen from this figure the SOI DV in both the X-direction and Y-direction is higher in most vehicles. Also, the DV decreases as the weight increases and the DV for SOI and Oblique are about the same for each vehicle. Figure 27 shows the AvgGs for the X-direction and Y-direction. In this figure it can be seen that oblique has a higher AvgGs when compared to SOI and the AvgGs decreases as vehicle weight increases. Also, figures demonstrate that the severity of the acceleration pulse when using an RMDB of constant closing speed is greater for smaller vehicles. Table A 3, Table A 4, Table A 5, Table A 6 gives all the calculated vehicle characteristics for both SOI and Oblique test in the New Model Tests.

Figure 28 shows the difference in the intrusion between SOI and oblique test. A negative intrusion means that the SOI test had higher intrusion than the oblique test for the same vehicle. It can be seen from this figure that the intrusion for the SOI test was not always the highest.

The next step is to compare the average vehicle characteristics from the crash test to the real-world. The only vehicle characteristics that can be compared are the frontal crush of the vehicle and interior intrusions. The real-world crush and interior intrusion was taken from the 276 drivers reported from Rudd et al. in 2011 [3]. The averages for the real-world included all DV and for the intrusions a value for IP had to be recorded to be included. Figure 29 and Figure 30 shows the average of the six crush points measured across the front of the vehicle for Oblique and SOI, respectively. For the Oblique it can be seen that the RMDBtV frontal crush was less than the real-world frontal crush. For the SOI tests the crush at C1 is the about the same but for the rest of the points the RMDBtV crush is higher. This could be due to the test parameters and the use of a homogenous barrier. Figure 31 shows that the RMDBtV tests do not produce as much IP intrusion as seen in the real-world data for both SOI and Oblique. However, the real-world data contains many older model vehicles. The 2010 and 2011 model year vehicles tested in the current fleet study could be expected to have improved or stiffer structures that would experience less intrusion compared to the prior model year vehicles, since these vehicles have been designed to the latest FMVSS and performed well in the latest consumer information program.

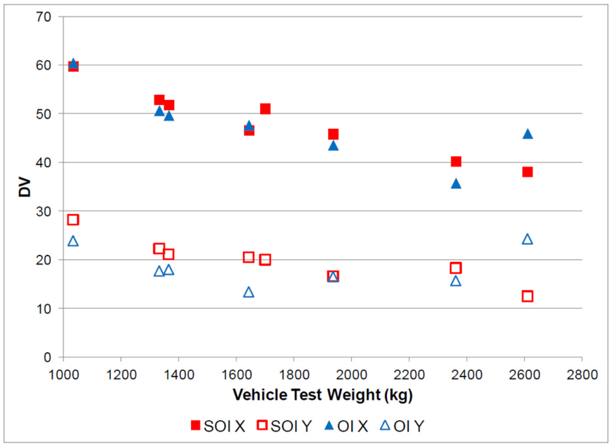

Figure 26. Comparison of DV for SOI and Oblique

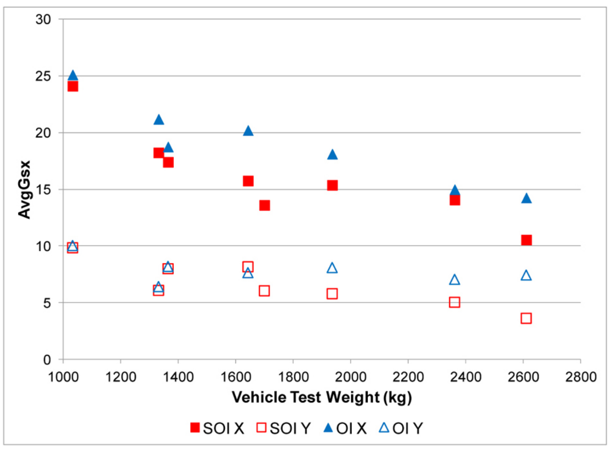

Figure 27. AvgGs

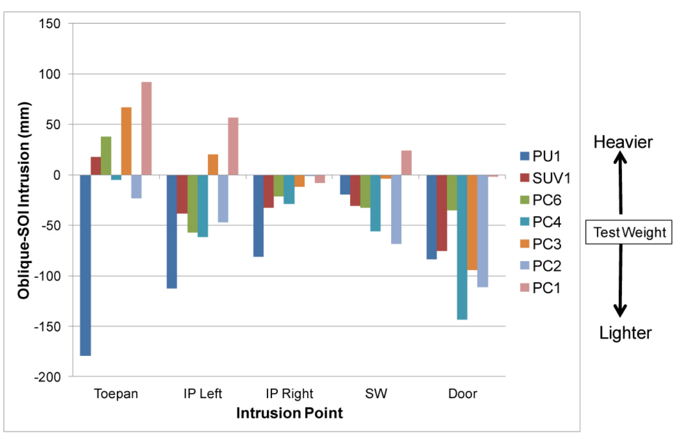

Figure 28. Difference in intrusion between Oblique and SOI intrusion points. A negative value indicates that intrusion in the SOI case is greater than intrusion in the Oblique case.

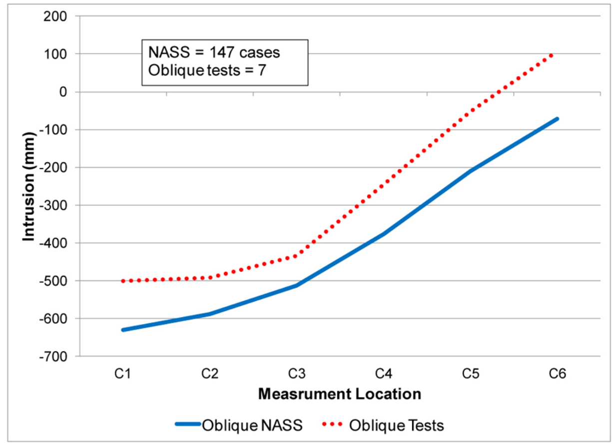

Figure 29. Average frontal crush comparison between NASS left offset and Oblique crash tests

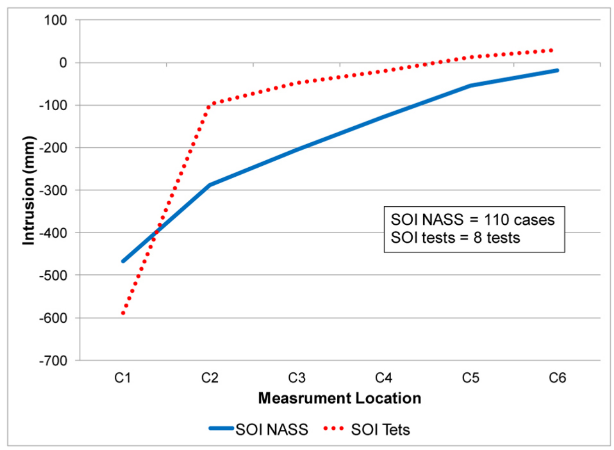

Figure 30. Average frontal crush comparison between NASS SOI cases and SOI crash tests

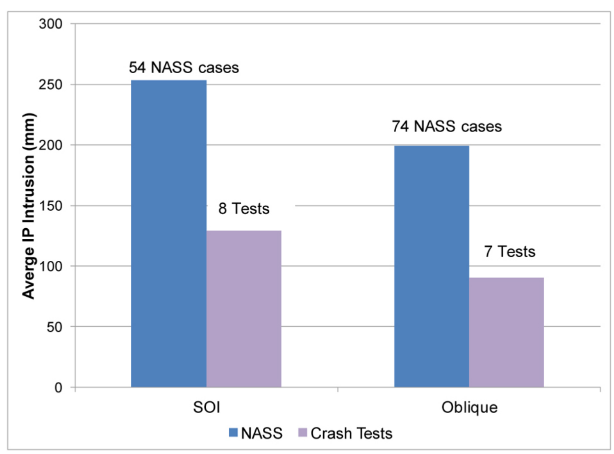

Figure 31. Average instrument panel intrusion comparison between NASS SOI cases and SOI crash tests

Rudd et al. (2011) [3] showed that there were no significant differences in injury patterns for oblique and SOI crash modes. From Figure 26 and Figure 27 it can be seen that there is only a slight difference in DV for both the Oblique and SOI, though Oblique tests demonstrated a marginally higher AvgGs for all vehicles. Based on a study by Saunders et al in 2007 [6], probability of injury can be predicted by the AvgGs measured in a test. A nonlinear relationship was developed between AvgGs and probability of injury based on a study of 408 New Car Assessment Program (NCAP) full-frontal tests. It should be noted that this relationship may be different in an SOI or oblique crash because of higher intrusions, the restraint system may not optimized for these test conditions and dummy kinematics when compared to the NCAP full-frontal test. Assuming that this relationship holds for SOI and oblique tests as well, the maximum difference in probability of injury between oblique and SOI tests is predicted to be roughly 9%. This is a similar magnitude to the difference in the incidence of injury shown by Rudd between SOI and left offset crashes, where chest injuries were 8% more frequent in left offset crashes. This finding shows that the injury probability demonstrated in these SOI and oblique tests agrees with the field data which suggests that there is not a significant difference in injury patterns between SOI and offset crash modes.

The main difference in vehicle response between the SOI and Oblique test modes is the magnitude of intrusion. Figure 32 and Figure 33 show the exterior crush of the PU1 in the oblique and SOI test, respectively. In the oblique test, the main longitudinal was engaged, and the bumper beam and longitudinal rail carried the load and prevented intrusion into the occupant compartment. In the PU1 SOI test, on the other hand, the main longitudinal rail was not engaged, and the suspension and tire were driven back into the occupant compartment. This demonstrates that the structural countermeasures may be different for these two different types of crashes. However, given similar DV and probability of injury predicted by AvgGs, the countermeasures for the restraint system may be the same.

Figure 32. PU1 oblique exterior crush

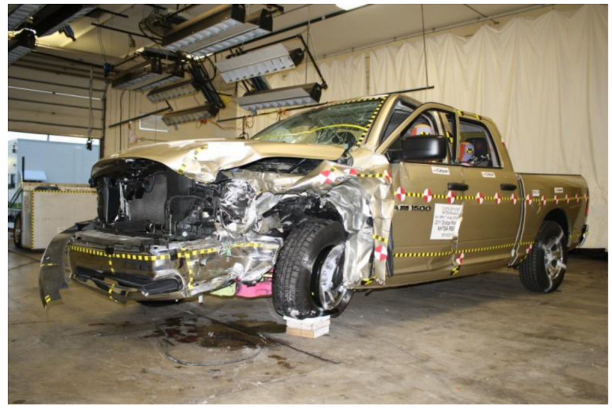

Figure 33. PU1 SOI exterior crush

Occupant Characteristics: New Vehicle Tests SOI and Oblique

The information collected in the fleet study provides an opportunity to evaluate the real-world applicability of the small overlap and oblique test procedure. The mod kit THOR-NT ATD was selected for use in this test procedure based on its superior biofidelity among the currently-available frontal ATDs. If this ATD is a proper surrogate for human occupants in a small overlap or oblique test procedure, it must accurately represent the occupant kinematics and injury risk that are present in the field.

One way to approach this comparison is to consider the contact locations and injuries witnessed in real-world small overlap and oblique crashes, as collected by Rudd et al (2011) [3]. Starting with the head, the most common sources of injury were interaction with the steering wheel, A-pillar, and air bag. In the fleet study tests, contacts occurred with the air bag in all cases, with isolated cases of contact with the A-pillar. There were no apparent contacts with the steering wheel, though this would not be expected in an oblique test condition when the occupant is placed in a well-defined initial seating position. The most frequent chest injury sources in the field were the belt, steering wheel, and door. Belt loading accounted for a majority of the chest deflection measured in this test series, along with isolated loading of the torso with the steering wheel in smaller vehicles. There were no apparent contacts between the torso and the door, though there was also no apparent intrusion of the door into the occupant compartment, so such contacts were not expected in the RMDB test procedure. The primary sources of KTH injury in the field were contact with the instrument panel, which occurred in both lower extremities in each of the tests in the field study.

Compared to the injury distributions shown in the field, the distribution of injury assessment values exceeding the provisional IARVs in the fleet study tests showed several similarities. For instance, Rudd et al in 2011 [3] showed that AIS 3+ head injuries occurred in roughly 20 percent of small overlap and left offset crashes. In the fleet study, 20 percent of the vehicles exceeded the IARV for the assessment of linear acceleration of the head. Similarly, 65 percent of the field cases showed AIS 3+ KTH injuries, while the acetabulum or femur injury risk was exceeded in 8 of the 15 fleet tests (53 percent). The tibia index IARV was exceeded in 40 percent of the fleet tests, a similar occurrence to the 38 percent of cases in the field that showed AIS 2+ leg and foot injuries. While more research is necessary to further develop injury risk functions for the THOR ATD necessary to provide more detailed injury assessment, these general trends suggest that the RMBDtV test procedure provides a viable representation of real-world occupant response.

While a methodology for the assessment of chest injury has not yet been developed for the mod kit THOR-NT ATD, the magnitudes of the chest deflection measured in this study are consistent with the magnitudes of deflection in belted PMHS tests that resulted in multiple rib fractures. In 2009, Shaw et al [16] published the thoracic response from a series of eight PMHS in belted, 40 km/h full-frontal sled tests in a passenger-side restraint system. The average deflections measured for the upper and lower left thoracic measurement sites, chosen to reproduce the THOR measurement locations, were 53.1 and 45.8 millimeters, respectively. These chest deflections resulted in at least two but as many as 27 rib fractures, as well as sternum fractures in all but one test and clavicle fractures in two of the tests. In the oblique and SOI fleet study, the average deflections of the upper and lower right measurement were 38 and 42 millimeters, respectively, with six of the tests exceeding the average PMHS deflection in the lower, under-the-belt measurement site. This suggests that at least two rib fractures would occur in six of the fifteen fleet tests (40%), which is similar to the incidence of injury seen in the field (45% occurrence of AIS3+ chest injuries per Rudd et al, 2011 [3]). However, such an estimate is limited pending the development of a chest injury risk function based on a wider variety of loading conditions, including air bags and force-limited belts.

Since the THOR ATD has not yet been described in the Code of Federal Regulations, there are some limitations associated with its application in the small overlap and oblique test series. First, the THOR ATD design has not yet been finalized, since as of November 2011 only two THOR-NT have been updated with the mod kit components and a full evaluation is underway. Second, injury risk functions applicable to the THOR ATD have not been fully developed, thus the injury assessment reference values used herein cannot be used to directly assess injury risk. This limitation is understood in that the injury assessment values collected have been used to make general observations and not quantitative injury risk calculations. Finally, as noted by Mueller et al in 2011 [17], the specific dummy used in this test series demonstrated a stiffer response to the thoracic certification procedure than the response specified in the THOR Certification Procedures Manual [18]. Were the THOR to meet the thoracic certification requirements, the chest deflections measured in these tests may have been greater, but due to the interaction of the torso with the steering wheel and the head with the air bag and side curtain, it is not possible to isolate the influence of chest stiffness on overall occupant kinematics.

SUMMARY/CONCLUSIONS

VTV VS. RMDB OBLIQUE COMPARISON

In general, the Oblique VtV to RMDBtV comparison showed the following:

- The RMDBtV acceleration pulse was similar in shape to the VtV acceleration pulse, though the magnitude was slightly higher, the peaks occurred earlier, and the duration of the pulse was shorter. These differences may make the RMDBtV demonstrate a slightly more severe vehicle and occupant response than the VtV tests, as demonstrated by the higher AvgGs.

- Additional evidence of the more severe response in the RMDBtV tests is demonstrated by higher peak belt loads and chest deflections than the corresponding VtV tests.

- The interior intrusions were similar with the exception of the A-pillar, which deformed more in the VtV tests.

- The occupant kinematics showed similar trends in the VtV and RMDBtV tests, though differences in the intrusion of the A-pillar and deformation of the door frame resulted in different head contact locations and severities.

NEW VEHICLE TESTS

In general, the New Vehicle Tests in both SOI and Oblique showed the following:

- The lightest vehicle had the highest total DV.

- While the DV for each vehicle pair was similar for both SOI and Oblique, the Oblique tests showed higher AvgGs than their SOI counterparts.

- There was no consistent relationship between intrusion and vehicle weight.

- Within vehicle pairs, the SOI condition did not always show greater intrusion than the Oblique condition.

- Three out of the fifteen tests in the New Model Study exceeded the head injury criterion. Head contact locations in the tests included the air bag, roof rail, and instrument panel, all of which have been identified as sources of head injuries in the field.

- The three tests with the highest toepan intrusion also showed the highest lower extremity injury risk, though there were also examples of high lower extremity injury risk with relatively low toepan intrusions.

REFERENCES

1. Bean, J. D., Kahane, C. J., Mynatt, M., Rudd, R. W., Rush, C. J., Wiacek, C., "Fatalities in frontal crashes despite seat belts and air bags." DOT HS 811 202, National Highway Traffic Safety Administration, Washington, DC, 2009.
2. National Highway Traffic Safety Administration, "Vehicle Safety Rulemaking and Research Priority Plan 2009-2011," Docket ID NHTSA-2009-0108-0023, National Highway Traffic Safety Administration, Washington, DC, 2009
3. Rudd, R., Scarboro, M., Saunders, J., "Injury Analysis of Real-World Small Overlap and Oblique Frontal Crashes," 22nd ESV Conference, Paper No. 11-0384, 2011.
4. Halloway, D., Saunders, J., Yoganandan, N., and Pintar, F., "An Operational Definition of Small Overlap Impact for Published NASS Data," SAE Technical Paper 2011-01-0543, 2011, doi: 10.4271/2011-01-0543.
5. Saunders, J., Craig, M.J., Suway, J., "NHTSA's Test Procedure Evaluations For Small Overlap/Oblique Crashes," 22nd ESV Conference, Paper No. 11-0343, 2011.
6. Saunders, J., Smith, D., and Barsan, A., "Restraint Robustness in Frontal Crashes," SAE Technical Paper 2007-01-1181, 2007, doi: 10.4271/2007-01-1181.
7. Eigen and Najm, "Problem Definition for Pre-Crash Sensing Advanced Restraints," DOT HS 811 114, 2009
8. Shams, T., Rangarajan, N., McDonald, J., Wang, Y., Platten, G., Spade, C., Pope, P., Haffner, M., "Development of THOR NT: Enhancement of THOR Alpha - the NHTSA Advanced Frontal Dummy," 19th ESV Conference, Paper No. 05-0455, 2005.
9. Trella, T., Samaha, R., Fleck, J., and Strassburg, G., "A Moving Deformable Barrier with Dynamic Force and Deflection Spatial Measurement Capabilities for Full Scale Tests," SAE Technical Paper 2000-01-0637, 2000, doi:10.4271/2000-01-0637.
10. Takhounts, E.G., Hasija, V., Ridella, S.A., Rowson, S., Duma, S., "Kinematic Rotational Brain Injury Criterion (BRIC)," 22nd ESV Conference, Paper No. 11-0263, 2011.
11. Dibb, A., Nightingale, R., Chauncey, V., Fronheiser, L., Tran, L., Ottaviano, D., Myers, B., "Comparative Structural Neck Responses of the THOR-NT, Hybrid III, and Human in Combined Tension-Bending and Pure Bending," Stapp Car Crash Journal, 50: 567-581, 2006.
12. Rupp, J.D., Flannagan, C.A., Kuppa, S.M., "Development of an injury risk curve for the hip for use in frontal impact crash testing," Journal of Biomechanics 34(3):527-531, 2010.
13. Martin, P.G., Scarboro, M., "THOR-NT: Hip Injury Potential In Narrow Offset And Oblique Frontal Crashes," 22nd ESV Conference, Paper No. 11-0234, 2011.
14. Kuppa, S., Wang, J., Haffner, M., Eppinger, R., "Lower Extremity Injuries and Associated Injury Criteria," 17th ESV Conference, Paper No. 456, 2001.
15. Ridella, S., Parent, D., "Modifications to Improve the Durability, Usability, and Biofidelity of the THOR-NT Dummy," 22nd ESV Conference, Paper No. 11-0312, 2011.
16. Shaw, G., Parent, D., Purtsezov, S., Lessley, D., Crandall, J., Kent, R., Guillemot, H., Ridella, S.A., Takhounts, E., Martin, P., "Impact Response of Restrained PMHS in Frontal Sled Tests: Skeletal Deformation Patterns Under Seat Belt Loading," Stapp Car Crash Journal, 53: 1-48, November 2009.
17. Mueller, B.C., Sherwood, C.P., Arbelaez, R.A., Zuby, D.S., Nolan, J.M., "Comparison of Hybrid III and THOR Dummies in Paired Small Overlap Tests," Proc. 55th Stapp Car Crash Conference, Dearborn, MI, November 2011.
18. National Highway Traffic Safety Administration, "THOR Certification Manual, Revision 2005.2," Report No: GESAC-05-04, U.S. Department of Transportation, Washington, DC, March 2005.

DEFINITIONS/ABBREVIATIONS

SA
sample abbreviations
UBT
use borderless table ≤ 3.5 inches wide

APPENDIX

APPENDIX A

Table A 1. X direction vehicle characteristics for the VtV and the RMDBtV PCb comparison

NHTSA Test Number	Test Type	Peak Gs	Peak Gs Time (ms)	$Duration_{-10Gs}$ (ms)	Total DV (kph)	DV_{-10Gs} (kph)	AvgGs
6831	VtV	36	51.8	90.8	56.5	50.1	15.6
7429	RMDBtV	38.5	44.3	69	53.7	46.5	19.1

Table A 2. Y direction vehicle characteristics for the VtV and the RMDBtV PCb comparison

NHTSA Test Number	Test Type	Peak Gs	Peak Gs Time (ms)	$Duration_{5Gs}$ (ms)	Total DV (kph)	DV_{5Gs} (kph)	AvgGs
6831	VtV	34.6	40.2	70.3	24.9	24.1	9.7
7429	RMDBtV	26	39.6	58.5	22.2	20.7	10

Table A 3. SOI X-direction vehicle characteristics

NHTSA Test Number	Model	Test Weight (kg)	Peak Gs	Peak Gs Time (ms)	$Duration_{-10Gs}$ (ms)	Total DV (kph)	DV_{-10Gs} (kph)	AvgGs	Time to -10 kph (ms)
7459	PC1	1033	61.2	18.7	70.2	63.8	59.8	24.1	16.4
7444	PC2	1332	63.4	34.5	82.1	57	52.9	18.2	30.7
7427	PC3	1365	46	36.6	84.4	56.4	51.9	17.4	32.1
7432	PC4	1643	40.7	38.6	83.9	54.9	46.7	15.8	31.5
7430	PC5	1700	36.5	55.4	106.3	55.1	51.1	13.6	40
7468	PC6	1936	32.3	44.8	84.5	49.9	45.9	15.4	34.7
7426	SUV1	2362	36.9	48	81	43.8	40.3	14.1	44.5
7456	PU1	2611	26.3	66.4	102.2	43.5	38.1	10.6	47.7

Table A 4. SOI Y-direction vehicle characteristics

NHTSA Test Number	Model	Test Weight (kg)	Peak Gs	Peak Gs Time (ms)	Duration5Gs (ms)	Total DV (kph)	DV5Gs (kph)	AvgGs	Time to 5 kph (ms)
7459	PC1	1033	25.2	38.8	81.1	32.7	28.2	9.8	19.7
7444	PC2	1332	30.7	64.6	103.7	22.4	22.3	6.1	40
7427	PC3	1365	27.1	57.5	74.7	22.1	21.1	8.0	37.1
7432	PC4	1643	18.2	57	71.1	20.7	20.5	8.2	32.2
7430	PC5	1700	23.9	44.2	93.6	22	20	6.1	45.2
7468	PC6	1936	18.8	46.1	81.1	18.7	16.6	5.8	42.2
7426	SUV1	2362	17.3	49.7	102.9	19.3	18.3	5.0	47.4
7456	PU1	2611	13.2	66.5	97.7	17	12.5	3.6	58.7

Table A 5. Oblique X-direction vehicle characteristics

NHTSA Test Number	Model	Test Weight (kg)	Peak Gs	Peak Gs Time (ms)	Duration-10Gs (ms)	Total DV (kph)	DV-10Gs (kph)	AvgGs	Time to -10 kph
7458	PC1	1033	44.4	41.2	68.2	64.7	60.5	25.1	15
7441	PC2	1332	53.8	35.2	67.7	54.2	50.7	21.2	26.1
7428	PC3	1365	37.6	36.2	75	52.5	49.7	18.8	26.5
7431	PC4	1643	36.9	40.95	66.8	50.5	47.7	20.2	20.7
7467	PC6	1936	33.8	48.2	68.1	45.7	43.6	18.1	27.2
7476	SUV1	2362	45.9	36.8	67.6	39.8	35.8	15.0	32.2
7457	PU1	2611	35.1	55.3	91.3	48.9	46.0	14.3	34.6

Table A 6. Oblique Y-direction vehicle characteristics

NHTSA Test Number	Model	Test Weight (kg)	Peak Gs	Peak Gs Time (ms)	Duration5Gs (ms)	Total DV (kph)	DV5Gs (kph)	AvgGs	Time to 5 kph
7458	PC1	1033	39.2	35.5	67.4	25.4	23.9	10.0	43.3
7441	PC2	1332	46.5	39.1	78.1	18.5	17.7	6.4	38.6
7428	PC3	1365	18.9	48.1	62.2	20.8	18.0	8.2	35.7
7431	PC4	1643	25.3	45	49.6	14.1	13.4	7.6	34.1
7467	PC6	1936	26.6	42.4	57.7	17	16.5	8.1	36.2
7476	SUV1	2362	18.9	47.35	63	17	15.7	7.1	40.9
7457	PU1	2611	38.4	63.5	92.5	24.5	24.3	7.4	61.5

APPENDIX B

The rotational brain injury criterion is calculated using the following formula:

$$BRIC = \frac{\omega_{\max}}{\omega_{cr}} + \frac{\alpha_{\max}}{\alpha_{cr}}$$

$$\begin{aligned}
&\text{where} \\
&\omega = \text{angular velocity at head CG} \\
&\alpha = \text{angular acceleration at head CG} \\
&\max = \text{maximum resultant value} \\
&cr = \text{critical value}
\end{aligned}$$

The critical intercepts for angular velocity and angular acceleration are unique to a given ATD. The process of developing these intercepts for the THOR dummy is described below:

1. Collect head acceleration data in various test conditions

a. Head CG acceleration (measured using tri-axial accelerometers)

b. Head CG angular velocity (either calculated using nine-accelerometer array or measured using angular rate sensors)

2. For each set of head kinematics collected in Step 1, run SIMon model (N=31)

a. Output: CSDM, ω, and α for each test

NHTSA Test #	Peak Linear Acc (G)	Peak Ang Acc (rad/s/s)	Peak Ang Vel (rad/s)	HIC15	CSDM
6830	107.3	10229	33.8	594	0.721
6831	64.0	3874	33.6	361	0.268
6852	52.0	4390	43.1	233	0.420
6855	37.0	3990	30.4	93	0.307
6872	38.9	2009	30.0	117	0.046
6873	80.8	3077	31.6	518	0.253
6937	108.9	8700	39.2	577	0.485
7144	98.7	7082	42.0	544	0.528
7145	63.3	6344	37.6	264	0.580
7292	90.3	6894	64.7	216	0.790
7293	136.2	10275	48.3	426	0.415
7366	58.0	4069	29.1	233	0.310
7368	83.8	5574	28.4	504	0.257
7371	94.0	7693	54.2	454	0.608
7429	355.0	18560	64.4	2523	0.712
7433	98.2	8390	41.1	270	0.509
7434	196.1	10388	37.4	1287	0.464
7428	108.5	11395	52.4	148	0.632
7431	52.9	3515	34.0	177	0.502
7427	198.0	16622	49.8	792	0.889
7432	44.0	5220	48.0	121	0.336
7430	64.7	5761	38.9	261	0.364
7426	41.3	4263	39.3	55	0.247
7458	66.3	5619	49.6	365	0.477
7441	254.6	14577	70.4	1570	0.803
7457	90.9	7270	46.2	457	0.559
7444	125.4	8468	52.1	338	0.537
7456	107.9	8731	28.8	179	0.238
7467	62.0	5384	54.7	120	0.556
7468	35.0	3548	41.6	93	0.214
7476	183.0	9484	41.5	704	0.525

3. Perform regression to relate BRIC to CSDM

a. Set constraint BRIC = 1, CSDM = 0.425 (represents 30% probability of DAI/AIS4+)

b. Optimize ω_{cr} and α_{cr} to maximize fit of linear equation: $BRIC = m \times CSDM + b$

c. ω_{cr} = 63.5 rad/s and α_{cr} = 19501 rad/s^2

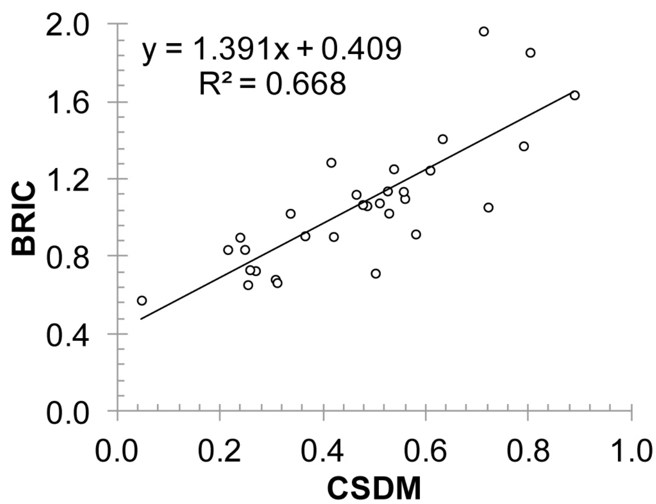

4. Determine CSDM relating to 30% risk of AIS 3+

a. Assuming equal severity ratios between HIC and BRIC, the relationship of AIS 4+ and AIS 3+ HIC injury risk curves was calculated to obtain the ratio (β_{34}) to relate similar injury probabilities. In other words, the ratio of the HIC that results in a 50% risk of

AIS 4+ injury to the HIC that results in a 50% risk of AIS 3+ injury is calculated. This ratio is applied to the CDSM AIS 4+ risk curve in order to calculate the CSDM AIS 3+ risk curve.

i.

$$\beta_{34} = \frac{HIC(50\% \text{ risk of AIS3}+)}{HIC(50\% \text{ risk of AIS4}+)} = \frac{CSDM(50\% \text{ risk of AIS3}+)}{CSDM(50\% \text{ risk of AIS4}+)}$$

ii.

$$Adj.CSDM = \frac{CSDM}{\beta_{34}}$$

iii.

$$P(AIS3+) = 1 - e^{\left(\frac{Adj.CSDM}{0.6162}\right)^{2.7667}}$$

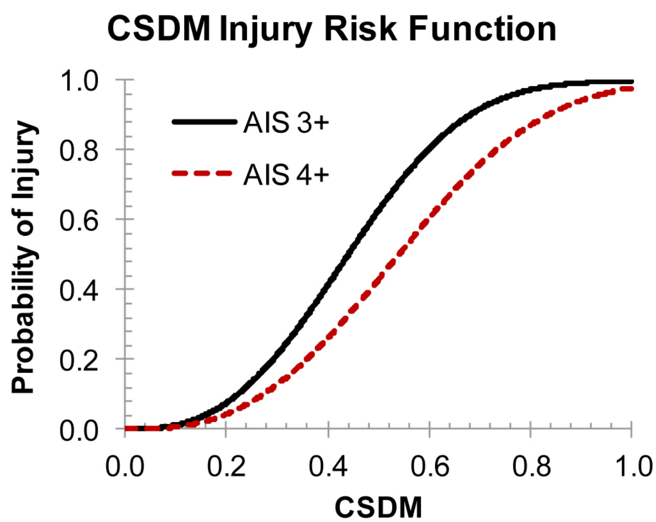

5. Calculate associated BRIC using equation in 3b

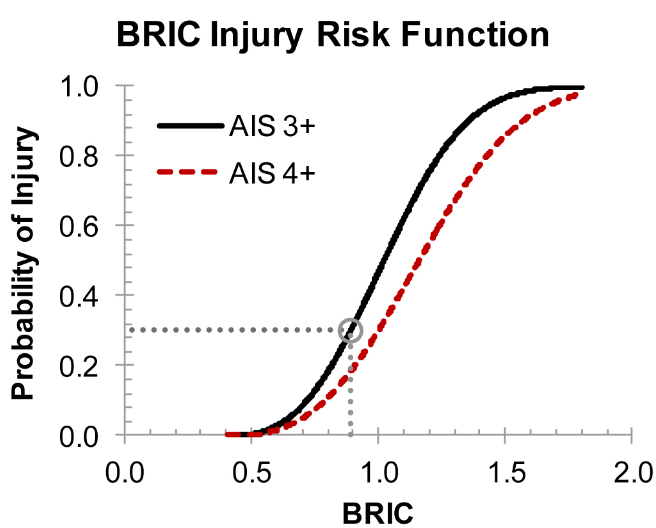

6. Solve for P ($AIS3+$) = 0.30; BRIC = 0.89